The role of *KMT2D* and *KDM6A* in cardiac development: A cross-species analysis in humans, mice, and zebrafish

Rwik Sen[1], Ezra Lencer[1,2], Elizabeth A. Geiger[3], Kenneth L. Jones[3#], Tamim H. Shaikh[3], and Kristin Bruk Artinger[1,*]

[1]Department of Craniofacial Biology, School of Dental Medicine, [2]Cell and Developmental Biology, [3] Department of Pediatrics, School of Medicine, University of Colorado Anschutz Medical Campus, Aurora, CO 80045, USA

*To whom all correspondence should be addressed

T: 303-724-4562 | F: 303-724-4580 | E: Kristin.Artinger@cuanschutz.edu

#Current address: Department of Cell Biology, Oklahoma University Health Sciences Center, Oklahoma City, OK 73104

Abstract

Congenital Heart Defects (CHDs) are the most common form of birth defects, observed in 4-10/1000 live births. CHDs result in a wide range of structural and functional abnormalities of the heart which significantly affect quality of life and mortality. CHDs are often seen in patients with mutations in epigenetic regulators of gene expression, like the genes implicated in Kabuki syndrome – *KMT2D* and *KDM6A*, which play important roles in normal heart development and function. Here, we examined the role of two epigenetic histone modifying enzymes, KMT2D and KDM6A, in the expression of genes associated with early heart and neural crest cell (NCC) development. Using CRISPR/Cas9 mediated mutagenesis of *kmt2d, kdm6a and kdm6al* in zebrafish, we show cardiac and NCC gene expression is reduced, which correspond to affected cardiac morphology and reduced heart rates. To translate our results to a human pathophysiological context and compare transcriptomic targets of *KMT2D* and *KDM6A* across species, we performed RNA sequencing (seq) of lymphoblastoid cells from Kabuki Syndrome patients carrying mutations in *KMT2D* and *KDM6A*. We compared the human RNA-seq datasets with RNA-seq datasets obtained from mouse and zebrafish. Our comparative interspecies analysis revealed common targets of *KMT2D* and *KDM6A*, which are shared between species, and these target genes are reduced in expression in the zebrafish mutants. Taken together, our results show that *KMT2D* and *KDM6A* regulate common and unique genes across humans, mice, and zebrafish for early cardiac and overall development that can contribute to the understanding of epigenetic dysregulation in CHDs.

Running Title:

Epigenetic regulation of cardiac development across zebrafish, mice, and humans

Key words:

Cardiac development, Kabuki Syndrome, epigenetics, cardiac neural crest cells, RNA sequencing, zebrafish, mice, human

Introduction

Heart disease is the leading cause of deaths in the United States and worldwide, and congenital heart defects (CHDs) are a leading cause of birth defect-associated infant illness and death (Benjamin et al., 2019; Gilboa, Salemi, Nembhard, Fixler, & Correa, 2010; Oster et al., 2013; Ottaviani & Buja, 2017). CHDs are present at birth, and they have a profound impact on the structure and function of an infantile heart. CHDs span a diverse spectrum of defects ranging from mild small atrial septal defects which heal on their own, to severe large ventricular septal defects which require medical intervention. In some cases, CHD-associated complications arise in adulthood, while for critical CHDs, surgery is required in the first year of life.

Significant gaps exist in our knowledge of the causes of CHDs, which may involve genetic, epigenetic, and environmental factors. Although epigenetic signatures like DNA methylation, histone modifications, chromatin remodeling, and microRNA have begun to be explored in CHDs and embryonic development in general, their underlying mechanisms in cardiogenesis are incompletely understood. Nonetheless, epigenetic modifications significantly contribute to the etiology and prognosis of CHDs and other developmental disorders because patients with same genotypes and syndromes often have large variations in phenotype, penetrance, and severity. Indeed, mutations in chromatin remodeler Chd7 and histone acetyltransferase Kat6a/b are associated with birth defects leading to Charge and Ohdo syndromes, respectively (Vissers et al., 2004) (Campeau et al., 2012).

Several studies have reported links between early heart development and two epigenetic modifiers - *KMT2D*, which methylates the histone H3K4 (histone 3 lysine 4), and *KDM6A*, which demethylates H3K27 (histone 3 lysine 27) (Ali, Hom, Blakeslee, Ikenouye, & Kutateladze, 2014; Hong et al., 2007; Koutsioumpa et al., 2019; Lan et al., 2007). Mutations in *KMT2D* and/or *KDM6A* result in Kabuki Syndrome (KS) where 28-80 % patients are afflicted with CHDs (Digilio et al., 2017) like atrial and ventricular septal defects, bicuspid aortic valves, aortic coarctation, double outlet right ventricle, transposition of great arteries, infundibular pulmonary stenosis, dysplastic mitral valve, Tetralogy of Fallot, etc. (Cocciadiferro et al., 2018; Digilio et al., 2017; Gazova, Lengeling, & Summers, 2019; Luperchio, Applegate, Bodamer, & Bjornsson, 2019; Shangguan et al., 2019; Tekendo-Ngongang, Kruszka, Martinez, & Muenke,

2019; Yap et al., 2020). Several variants and missense mutations of *KMT2D* and *KDM6A* have been identified in KS and other novel syndromes (Cocciadiferro et al., 2018; Cuvertino et al., 2020; Xin et al., 2018). In addition to CHDs, KS patients have typical dysmorphic features like long palpebral fissures with eversion of lateral third of the lower eyelid, arched and broad eyebrows with notching or sparseness of lateral third, short columella with depressed nasal tip, prominent or cupped ears, and persistent fingertip pads (Adam et al., 2019).

Recent studies have significantly contributed to our understanding of cardiac development and function as regulated by *KMT2D* and *KDM6A* (Ang et al., 2016; Lee, Lee, & Lee, 2012; Schwenty-Lara, Nurnberger, & Borchers, 2019; Serrano, Demarest, Tone-Pah-Hote, Tristani-Firouzi, & Yost, 2019). *KMT2D* or lysine-specific methyltransferase 2D, is also known as *MLL2* or myeloid/lymphoid or mixed-lineage leukemia 2. It belongs to a family of 7 SET1-like histone methyltransferases (Ali et al., 2014). KMT2D contains a SET domain for histone methylation, PHD and coiled-coil domains, and zinc finger domains. *KDM6A* (and *kdm6l* in zebrafish) or Lysine Demethylase 6A, is also known as *UTX* or Ubiquitously transcribed tetratricopeptide repeat, X chromosome. UTX, UTY and JMJD3 comprise a subfamily of proteins containing JmjC-domain (Jumonji C) and zinc fingers, and they are evolutionarily conserved from *Caenorhabditis elegans* to human (Klose, Kallin, & Zhang, 2006; Lan et al., 2007; Shi & Whetstine, 2007). The JmjC-domain is associated with histone demethylation (Accari & Fisher, 2015), while the tetratricopeptide repeats at N-terminal regions of UTX and UTY are predicted protein interaction motifs (Lan et al., 2007). It is important to note that *KDM6A* or *UTX* is an X-linked gene, with 2 copies in females (XX) and 1 copy in males (XY), where the Y chromosome has the homolog, *UTY* (Itoh et al., 2019). Studies indicate that *UTY* and *UTX* diverged from a common ancestor, yet the functional role of *UTY* in histone demethylation needs further investigation, because some studies show that it has a lower histone demethylation activity than *UTX* (Faralli et al., 2016; Hong et al., 2007; Itoh et al., 2019; Lan et al., 2007; Shpargel, Starmer, Wang, Ge, & Magnuson, 2017; Shpargel, Starmer, Yee, Pohlers, & Magnuson, 2014; Walport et al., 2014).

To elucidate the roles of *KMT2D* and *KDM6A* in heart and overall development, we performed an inter-species comparison of common gene targets of *KMT2D* and *KDM6A* from zebrafish, mice, and human RNA-seq datasets, and an *in vivo* analysis of mutations in zebrafish

genes *kmt2d, kdm6a* and its paralog *kdm6al,* during early development. We mutated *kmt2d, kdm6a* and *kdm6al* by CRISPR/Cas9 mutagenesis, while the human data are derived from RNA-sequencing analysis of two patients with Kabuki Syndrome (KS). One of the KS patients has a T to C substitution at position 4288 in *KMT2D* cDNA, resulting in C to R amino acid change at position 1430, while the other patient has a 3.2-MB microdeletion on the X chromosome (chrX:43620636-46881568) leading to a deletion of *KDM6A* (Van Laarhoven et al., 2015). Our results reveal that some of the genes which are involved in cardiogenesis, cardiac function, vasculature, neurogenesis, and overall development, are regulated by *KMT2D* and *KDM6A* across zebrafish, mice, and humans. Our *in vivo* analysis in CRISPR-mutated zebrafish indicate that *kmt2d* and *kdm6a* regulate genes involved in early embryonic, cardiac, and neural crest cell (NCC) development. Although the mechanism of the phenotypes are yet to be elucidated, our results corroborate current findings in the field, and present a pan-species perspective of the roles of *KMT2D* and *KDM6A* in heart and overall development. The study strengthens the establishment of zebrafish as a model to study CHDs resulting from KS and epigenetic dysregulation, and identifies genes targeted by *KMT2D* and *KDM6A* across humans, mice, and zebrafish, which can serve as either potential biomarkers or therapeutic targets in heart disease.

Materials and Methods

Animals

Zebrafish were maintained as previously described (Westerfield, 2000). Embryos were raised in defined Embryo Medium at 28.5°C and staged developmentally following published standards as described (Kimmel, Ballard, Kimmel, Ullmann, & Schilling, 1995). The Institutional Animal Care and Use Committee of the University of Colorado Anschutz Medical Campus approved all animal experiments performed in this study, and conform to NIH regulatory standards of care.

Genotyping

For fish, fin clips, single whole embryos or single embryo tails were lysed in Lysis Buffer (10 mM Tris-HCl (pH 8.0), 50 mM KCl, 0.3% Tween-20, 0.3% NP-40, 1 mM EDTA) for 10

minutes at 95° C, incubated with 50 ug of Proteinase K at 55°C for 2 hours, followed by another incubation at 95°C for 10 minutes. For genotyping *kmt2d* mutants, the following primers were used (F) 5'- AACAGAGGCAGTACAAAGCCAT-3' and (R) 5'-TTGTTGTTGCATCAATAGGTCC-3'. The 300 bp PCR product was run out on a high percentage (4%) agarose gel to distinguish homozygous mutant embryos from heterozygous and wildtype embryos. This 300 bp PCR product was diluted 1:100 in nuclease-free water. A second set of primers was designed using dCAPS Finder 2.0 (http://helix.wustl.edu/dcaps/) to generate a primer containing a mismatch that creates a restriction endonuclease site based on the identified SNP mutation in the *kmt2d* mutant allele. Using above forward primer and (R) 5'-GCATTCCTACTGCCGAAGCATCAAGAGAAG -3', a PCR product was generated that was then digested using the restriction enzyme, MboII, which digests the wildtype sequence but is unable to cut the mutant sequence, allowing for homozygous mutant embryos to be distinguished from heterozygous and wildtype embryos. For *kdm6a*, the genotyping primers are (F) 5'-ATGAAATCGTGCGGAGTGTCGGT-3' and (R) 5'-ATAGAGGACAACACAGGCGGTTC-3'. For dCAPS, above forward primer and (R) 5'-CTGCAATCATTTGCACCGCTTTGAGCAT-3' are used, followed by restriction enzyme SphI. For *kdm6al*, the genotyping primers are (F) 5'- GGCTTTTATTGTGGCTTTTGGAC-3' and (R) 5'-AACTATCAAAAGCGCAGAAGCC-3'. For dCAPS, (F) 5'-GAGGAGAAGAAAATGGCGGCG GGAAAAGCGAGTGAACTCGA -3', above reverse primer, and restriction enzyme is XhoI are used.

Generation of Zebrafish Mutant Lines

Zebrafish mutant lines for *kmt2d* and *kdm6a* and *kdm6al* (*kdm6a/l*) were generated via CRISPR-based mutagenesis. CRISPR target sites were identified using Zifit Targeter http://zifit.partners.org/ZiFiT/ and CHOPCHOP https://chopchop.cbu.uib.no/. Selected targets were used to generate guide RNAs (gRNAs) specific for *kmt2d* or *kdm6a*. gRNAs were prepared as previously described (Gagnon et al., 2014). Prepared gRNAs were then co-injected with 600 ng/ul of Cas9 Protein (PNA bio) and 200 mM KCl. Cas9/sgRNA complexes were formed by incubating Cas9 protein with sgRNA at room temperature for 5 minutes prior to injecting into the cytoplasm of wild-type zebrafish embryos at the 1-cell stage. Mosaic germline founders were identified by screening the progeny of CRISPR injected fish grown to adulthood. Two

separate alleles were identified for each single mutant gene, and we focused on the alleles schematized in Figure 1. The *kmt2d* and *kdm6a/l* mutant alleles are predicted frameshift mutations that interrupt the coding sequence upstream of the SET and JmjC domains, respectively, which are responsible for functional histone methyltransferase and demethylase activities in the corresponding genes.

In situ hybridization

Zebrafish embryos were collected at 48 hours post fertilization and fixed in 4% paraformaldehyde overnight and dehydrated in methanol. Following rehydration in methanol gradients, embryos were bleached (3% hydrogen peroxide and 0.5% potassium hydroxide) until body pigment cells and the eyes were visibly cleared (10 minutes), digested with proteinase K for 8 minutes and fixed in 4% paraformaldehyde for 25 mins at 4°C. Embryos and DIG-labeled probes (*sox10, foxd3, crestin, hand2a, mef2ca, kmt2d, kdm6a, kdm6al*) were prehybridized for 2-4 hours at 65°C before incubating embryos with the indicated probes overnight at 65°C. Embryos were subjected to a series of stringency washes in a wash buffer containing 50% formamide, 2X SSC pH 4.5, and 1% SDS before blocking in a buffer containing 2% Blocking Reagent (Roche) and 20% Heat-Inactivated sheep serum diluted in 1X MABT (100 mM maleic acid, 150 mM NaCl, 0.1% Tween-20) and anti-DIG antibody (Roche) incubation overnight at 4°C. After another set of stringency washes in NTMT (100 mM NaCl, 100 mM Tris pH 9.5, 50 mM $MgCl_2$, 1% Tween-20), embryos were developed with BM purple reagent (Roche) and stored in PBS.

RNA isolation and qPCR

Total RNA was isolated from *kmt2d-/-*, *kdm6a-/-*, and wildtype 48 hpf embryos with TRIzol reagent (Invitrogen) and pheno/chloroform. RNA (1-1.5 μg) was reverse transcribed to complementary DNA (cDNA) with SuperScript III First-Strand Synthesis cDNA kit (Invitrogen). Using Roche FastStart Universal Probe Master (Rox) (Catalog# 4914058001), real-time semiquantitative PCR (qPCR) was performed in Applied Biosystems StepOne Plus, with the following primers:

sox12 Pr#6 F: 5' tgacttgcaccacaactgct 3'

R: 5' gcaactcaccaattcctgct 3'

slc22a23 Pr#56 F: 5' ggcagtgatagtctgccctct 3'

R: 5' gcagagactcgggaaaagc 3'

foxp4 Pr#68 F: 5' gacaaggcctggtgaaccta 3'

R: 5' tgctgcaggctctgaatg 3'

nr2f6a Pr#2 F: 5' aaggccatagcgctcttct 3'

R: 5' ctcggtaagagccacctgag 3'

six3a Pr#67 F: 5' aacaggagacaacgagacagg 3'

R: 5' gccattctgccctattgct 3'

id3 Pr#25 F: 5' gctatgtgccattaggatgga 3'

R: 5' ggctcacccttcactctct 3'

prdm1a Pr#66 F: 5' ccacattgccaccacaacta 3'

R: 5' gtagcccttgaggtggaacc 3'

anxa4 Pr#68 F: 5' agaggatgatgcccagaaaa 3'

R: 5' atgatagtcgcctcgttggt 3'

Pr followed by the number represents probe numbers from Roche Universal Probe Library. Transcript levels were normalized to *actb1* as reference gene, (F): 5'-GGCAGCGATTTCCTCATC-3', and (R):5'-TCACTCCCCTTGTTCACAATAA-3'. Transcript abundance and relative fold changes in gene expression were quantified using the $2^{-\Delta\Delta Ct}$ method relative to control.

Western Blot

For western blotting, 30 to 40 zebrafish embryos of each genotype were collected and pooled at 48 hpf. Embryos were incubated on ice for 5 minutes. Calcium-free Ginzberg Fish Ringer's solution (NaCl, KCl, NaHCO3) was added to the embryos for deyolking. Samples were centrifuged for 1.5 minutes at 5000 rpm. Pellets were washed in deyolking wash buffer (NaCl, Tris (pH 8.5), KCL and $CaCl_2$). Samples were again centrifuged for 1.5 minutes at 5000 rpm. All liquid was removed, and pellet was resuspended and lysed in SDS sample buffer (0.1% glycerol, 0.01% SDS, 0.1 M Tris (pH 6.8)) for at least 10 minutes on ice. Embryos were homogenized in lysis buffer and briefly centrifuged. Total protein concentrations were determined with the Bio-Rad Dc Protein assay. Proteins (20 ug) were separated by SDS-PAGE (12%) and transferred to polyvinylidene difluoride membranes. Membranes were blotted using antibodies for H3K4me3 (Abcam, ab8580), H3K27me3 (Abcam, ab6002) and H3 (Cell

Signaling Technology, 9715S), and secondary antibodies i.e. goat anti-rabbit for H3K4me3 and H3, and goat anti-mouse for H2K27me3, conjugated with HRP (horseradish peroxidase). Chemiluminescent detection was performed with Luminata Classico Western HRP Subtrate (Millipore) and imaged on a BioRad Chemidoc multiplex imager.

Whole Mount Immunofluorescence

Zebrafish embryos were collected at the indicated timepoint and fixed in 4% paraformaldehyde overnight at 4°C embryos were washed and dehydrated through a graded methanol series. Samples in 100% methanol were incubated at least overnight in methanol prior to the next steps. Following rehydration through the reverse methanol gradient, embryos were washed in 1x Phosphate Buffered Saline (PBS, pH 7.3) with 0.1% Tween 3 times for 10 minutes at room temperature, then equilibrated in 150 mM Tris pH 9.5 for 5 minutes at room temperature before a 20 minute incubation in the Tris solution at 70°C. Following this retrieval step, embryos were washed 3 times for 10 minutes each in PBS with 0.1% Tween at room temperature then 2 times for 5 minutes in distilled water before blocking at room temperature in blocking solution containing 10% normal goat serum and 1% bovine serum albumin in PBS. Embryos were then incubated in primary antibodies for 3 days at 4°C. Primary antibodies anti-MF20 and anti-GFP (Life Technologies, Conjugate Alexa Fluor® 488 A-21311), were diluted in blocking solution. For anti-MF20, we acknowledge the Developmental Studies Hybridoma Bank (DSHB) at the University of Iowa, and Dr. Donald Alan Fischman for depositing MF20 to DSHB (DSHB Hybridoma Product MF 20, Antibody Registry ID: AB_2147781). Following primary antibody incubation, samples were washed thoroughly in PBS with 0.1% Triton X-100. Next, samples were incubated in fluorescently tagged goat anti-mouse 594 secondary antibody (Invitrogen, A-21044) for 2 days at 4°C. After secondary antibody incubation, embryos were washed thoroughly in PBS with 0.1% Triton X-100 before incubating in DAPI diluted in PBS for 1 hour at room temperature. Samples were quickly washed in PBS and passed through a glycerol/PBS gradient before mounting on glass slides. Embryos were imaged on a Leica TCS SP8 confocal microscope. Images were processed in LASX software and quantification of cell numbers were completed on max projections of z-stack images using Image J.

Human Cell Samples

Patient-derived lymphoblastoid cell lines (LCLs) used in this study were previously generated from KS patients with mutations in *KMT2D*/*MLL2* and *KDM6A* (Van Laarhoven et al 2015). Control LCLs from age and demography-matched subjects, were obtained from the Coriell Institute for Medical Research https://www.coriell.org/

RNAseq of human Kabuki Syndrome patients and comparison across taxa

Human LCLs from *KMT2D* and *KDM6A* patients and controls, as mentioned above, were grown to a count of 10^6 and pelleted. RNA was extracted by Zymo Research Direct-zol™ RNA MiniPrep kit (Catalog #R2050). Two cDNA libraries for each genotype (e.g. wildtype, *KMT2D* mutant, *KDM6A* mutant) were prepared from separate RNA MiniPreps using the Nugen mRNA kit for Illumina sequencing. Sequencing was perfomed on an Illumina NovaSEQ6000 (150bp paired-end reads) at the Genomics and Microarray Shared Resource Core Facility at University Of Colorado Denver Cancer Center. Libraries were sequenced to an average depth of 42 million reads. Reads were aligned to the human genome (hg38) using STAR Aligner (v2.7.3a) (Dobin et al., 2013), and gene counts were computed from STAR using quant mode (Dobin et al., 2013). Differential expression was performed in R using Deseq2 (Love, Huber, & Anders, 2014).

We compared our human RNAseq data to previously published datasets of KMT2D and KDM6A mutants from mice and zebrafish (Ang et al., 2016; Fahrner et al., 2019; Itoh et al., 2019; Lei & Jiao, 2018; Serrano et al., 2019; Shpargel et al., 2017). RNAseq datasets were downloaded from the NCBI Gene Expression Omnibus. Datasets included GSE129365 (Kmt2d mouse chondrocytes, (Fahrner et al., 2019)), GSE103849 (Kdm6a mouse neural crest cells, (Shpargel et al., 2017)), GSE121703 and GSE128615 (mouse Cd4 cells, (Itoh et al., 2019)), GSE110392 (mouse neural stem cells, (Lei & Jiao, 2018)). In addition an RNAseq dataset of whole embryo zebrafish Kmt2d mutants was provided by Serrano et al. (Serrano et al., 2019).

Where necessary, downloaded RNAseq datasets were re-analyzed using DESeq2 for differential expression.

To identify potential core genes regulated by Kmt2d and Kdm6a we found the intersection set of genes differentially expressed at a nominal p-value of 0.05 in each dataset for all Kmt2d and Kdm6a RNAseq datasests respectively. To do this, we used BioMart as implemented in R to convert non-human gene symbols into orthologous human ensembl identifiers, while allowing multiple mappings to account for gene duplications. Intersection sets were computed from these human ensemble identifiers.

Statistical Analysis

Data shown are the means ± SEM from the number of samples or experiments indicated in the figure legends. All assays were repeated at least three times with independent samples. *P* values were determined with Student's *t* tests using GraphPad Prism.

Results

Disruption of *kmt2d* and *kdm6a/l* in zebrafish causes cardiac defects.

We disrupted *kmt2d, kdm6a* and *kdm6al* in zebrafish by CRISPR/Cas9 mutagenesis to understand their roles in cardiac development. Guide RNAs were designed to target a Protospacer Adjacent Motif (PAM) site in exon 6 of *kmt2d*, and exon 1 of *kdm6a and kdm6al* (Figure 1A-C). Mutations in ORF (open reading frame) sequences for *kmt2d*, *kdm6a*, and *kdm6al* are shown in Figure 1A-C. *kmt2d*^{CO1015}, *kdm6a*^{CO1016}, and *kdm6al*^{CO1017} are used in the study, hereafter referred to as *kmt2d*-/-, *kdm6a*-/-, and *kdm6al*-/- mutants, respectively. Although mutations in *kmt2d* alleles are located in a downstream exon, the resulting mutations are predicted to be loss-of-function alleles, similar to mutations in *kdm6a* and *kdm6al*. The mutations were further verified by reduced expression of the transcript for each allele in each of the corresponding mutants at 48 hpf, following *in situ* hybridization with probes made from cDNA for *kmt2d*, *kdm6a* and *kdm6al*. In wildtype embryos, *kmt2d, kdm6a*, and *kdm6al* are strongly

expressed in the brain, eye and broadly in the rest of the body, including the heart consistent with previous reports (Van Laarhoven et al., 2015) (Figure 1D). The expression for *kmt2d*, *kdm6a* and *kdm6al* in the corresponding mutants is reduced, however, expression in the notochord appears to be non-specific. To examine the effect of each mutation on histone modifications, we probed for H3K4me3 and H3K27me3 by western blot in 48 hpf whole embryos as compared to total histone3 (H3) levels. Consistent with the role of Kmt2d in promoting H3K4me3 (Koutsioumpa et al., 2019), we observed a reduction in the overall levels of H3K4me3 in *kmt2d-/-* zebrafish at 48 hpf (Figure 1E). Likewise, mutation of *kdm6a* and its zebrafish paralog *kdm6al*, led to elevated H3K27me3 at 48 hpf as compared to total H3 (Figure 1E) (Hong et al., 2007).

To study the roles of *kmt2d* and *kdm6a/kdm6l* in heart development, we analyzed zebrafish heart formation in the *cmlc2*:GFP (coldheart) background at 48 hpf. *cmlc2* is the cardiac myosin light chain 2 gene which marks the myocardium (Huang, Tu, Hsiao, Hsieh, & Tsai, 2003), and its expression results in a fluorescent heart. We used an antibody against sarcomeric myosin heavy chain (MF20), which is expressed in cardiomyocytes (George, Colombo, & Targoff, 2015) in the *cmlc2*:GFP background to analyze cardiac morphology. We observed altered cardiac morphology of mutants (Figure 1 F), with *kmt2d* and *kdm6a* mutants presenting with altered chamber morphology as compared to wildtype. In addition, all have a small but statistically significant reduction in heart rates (Figure 1G) but not in the total area of the heart (Supplemental Figure 1). Hence, as previously observed in KS patients and the previous animal studies, single mutations in *kmt2d*, *kdm6a* and *kdm6al* cause defects in cardiac development to varying levels.

Cardiac and neural crest cell gene expression is reduced in *kmt2d* and *kdm6a/l* mutant embryos.

Development of the heart occurs earliest among all other functional organs when the cardiac crescent begins forming with contributions from cardiogenic progenitor cells post-gastrulation (Herrmann, Gross, Zhou, Kestler, & Kuhl, 2012). Subsequently, the cardiogenic mesoderm gives rise to the first heart field (FHF) and second heart field (SHF) (Herrmann et al., 2012; Moretti et al., 2006; L. Yang et al., 2008). The FHF contributes to the primary heart tube,

left ventricle, and most of the atria, while SHF contributes to right ventricle, outflow tract and atria (Buckingham, Meilhac, & Zaffran, 2005; Herrmann et al., 2012; Laugwitz, Moretti, Caron, Nakano, & Chien, 2008). Orchestrated signals from mesoderm-derived FHF and SHF, as well as endoderm, are crucial for cardiogenesis (Herrmann et al., 2012). Hence, we tested for the expression of *hand2* and *mef2ca* which are expressed in both FHF and SHF (Herrmann et al., 2012), in *kmt2d*, *kdm6a* and *kdm6al* mutants by *in situ* hybridization at 48 hpf. *hand2a*, or *h*eart *a*nd *n*eural crest *d*erivatives expressed *2a*, is a basic helix-loop-helix transcription factor that regulates cardiac morphogenesis, cardiomyocyte differentiation and cardiac-specific transcription and is expressed in the FHF and neural crest in the pharyngeal arches (McFadden et al., 2005; Schindler et al., 2014). *hand2a* belongs to an evolutionarily conserved cardiac transcription program which specifies cardiac progenitors in the anterior lateral plate mesoderm (ALPM), which migrate to the midline of the embryo for expression of cardiac sarcomere proteins, ultimately fusing to generate a beating heart tube (Lu, Langenbacher, & Chen, 2016). *hand2a* expression domains demarcate the heart forming region in ALPM (Lu et al., 2016; Schoenebeck, Keegan, & Yelon, 2007), and it specifies major domains which pattern pharyngeal arches of zebrafish dorsoventral axis (Talbot, Johnson, & Kimmel, 2010). In zebrafish heart primordium, *hand2a* expression domains appear anterior-lateral to hindbrain rhombomere 3 (Maves, Tyler, Moens, & Tapscott, 2009). Expression of *hand2a* are reduced in the *kmt2d, kdm6a and kdm6al* mutants (Figure 2). *hand2a* is normally expressed broadly in the heart is reduced especially in the midline in *kmt2d* and *kdm6a* mutants, but lesser extent in *kdm6al*-/-. A similar pattern of expression is observed for *mef2ca*, or *m*yocyte *e*nhancer *f*actor *2ca*, expressed primarily in the forming heart region, is a transcription factor that regulates myocardial differentiation and cardiac development (Hinits et al., 2012). In zebrafish hearts, *mef2ca* is expressed in the ALPM from 6 somite stage and persists during the fusion of the two heart fields into the primitive heart tube (Hinits et al., 2012). Expression of *mef2ca*, is similarly downregulated in the heart region of *kmt2d, kdm6a and kdm6al* mutants. Hence, *kmt2d, kdm6a and kdm6al* regulate genes involved in early events of heart development.

In addition to the cardiogenic mesoderm, cardiac development is also regulated by cardiac NCCs which contribute to outflow tract septation, aortic arch patterning, and semilunar valves (Brade, Pane, Moretti, Chien, & Laugwitz, 2013). Previous studies have indicated that *kmt2d* and *kdm6a* plays a role in regulating NCC formation (Schwenty-Lara, Nehl, & Borchers,

2019; Shpargel et al., 2017). To further investigate the roles of *kmt2d* and *kdm6a* we analyzed the expression of early neural crest-specific markers like *sox10*, *foxd3*, and *crestin* in zebrafish by *in situ* hybridization. *sox10* regulates the formation of NCCs from the time of their emergence, and specifies several derivatives of NCCs (Aoki et al., 2003; Dutton et al., 2001; Southard-Smith, Kos, & Pavan, 1998). *foxd3* is expressed in NCCs and maintains NCCs progenitors (Labosky & Kaestner, 1998; Teng, Mundell, Frist, Wang, & Labosky, 2008). *crestin* is characterized by pan-neural crest expression during zebrafish embryogenesis including premigratory and migrating NCCs (Luo, An, Arduini, & Henion, 2001; Rubinstein, Lee, Luo, Henion, & Halpern, 2000). In *kmt2d*, *kdm6a and* kdm6a*l* mutant zebrafish, the expression of *sox10* is slightly reduced in all three mutants at 12 hpf suggesting a reduction in NCC induction. The expression of *foxd3* at 15 hpf is also reduced specifically in the anterior most population migrating to the heart in *kmt2d* and *kdm6a* but not in *kdm6al* mutants. The overall expression of *crestin* at 24 hpf is not markedly reduced in any of the mutants which indicates normal NCC migratory streams (Figure 3). These results show that *kmt2d* and *kdm6a* regulate early stages of NCCs development in zebrafish.

Comparative analysis reveal common targets of *KMT2D* and *KDM6A*

To translate our results into the context of human health, we investigated the transcriptome of 2 human Kabuki Syndrome patients carrying mutations in *KMT2D* and *KDM6A*, by RNA sequencing of their lymphoblastoid cells. The patient with *KMT2D* mutation has a transition c.4288T>C (p.C1430R) (Figure 4A) and the patient with *KDM6A* mutation has a microdeletion in chromosome X resulting in a deletion of *KDM6A* (Figure 4A Table). As controls, we used LCLs from age and ethnicity matched individuals. To ascertain differential gene expression, generated reads from RNA-seq were mapped to the human genome using STAR aligner (Dobin et al., 2013) and differential expression was performed in R with DESeq2. Differentially expressed genes (nominal p value <= 0.05) from our *KMT2D* human dataset were compared to RNA sequencing datasets for *Kmt2d*-mutant mice and zebrafish generated by other researchers (see methods). For mice, the RNA sequencing dataset is derived from embryonic hearts (Ang et al., 2016), and the zebrafish data are obtained from whole embryos (Serrano et al., 2019). Likewise, our *KDM6A* human RNA seq datasets were compared to three distinct RNA seq datasets of mice that are mutant for *Kdm6a*. The mice datasets are derived from NCCs

(Shpargel et al., 2017), neural stem cells (Lei & Jiao, 2018), and CD4+ cells (Itoh et al., 2019). For *KDM6A*, the comparison is only between humans and mice, since zebrafish RNA sequencing for *kdm6a* mutation are not available.

A comparison between datasets from the 3 species revealed 76 common targets for *KMT2D* (Figure 4B). 30 of the 76 common targets are either upregulated or downregulated in a similar pattern across the 3 species, while 46 do not share a similarity in expression patterns among the 3 species, as shown by heat maps (Figure 4C). For *KDM6A*, 7 common targets were found between human and the 3 mice datasets (Figure 5A). The variation in the number of common targets between *KMT2D* and *KDM6A* datasets could partly be due to the differences in the roles and targets of *KMT2D* and *KDM6A*, as well as functional redundancy of other family members across species (Akerberg, Henner, Stewart, & Stankunas, 2017; Crump & Milne, 2019; Fellous, Earley, & Silvestre, 2019; Nottke, Colaiacovo, & Shi, 2009). Heat maps show that out of the 76 common targets between the 3 species, expression patterns of 49 genes are similar between mouse and human datasets, while 27 genes are not (Figure 5B). The dissimilarity is probably due to differences in cell type and age. Hence, like *KMT2D*, *KDM6A* also likely regulates gene expression through a tight temporal and spatial orchestration.

We selected common targets for both *KMT2D* and *KDM6A* datasets, based on their roles in cardiac and overall development as summarized in Tables 1 and 2, to validate whether these genes are similarly regulated by *kmt2d* or *kdm6a* during early development in zebrafish. The genes selected from analysis of *KMT2D* datasets are *SOX12*, *SLC22A23*, *FOXP4*, *NR2F6*, and *SIX3*. The genes selected from analysis of *KDM6A* datasets are *ID3*, *PRDM1*, and *ANXA4*. For validation, we performed qRT-PCR for *sox12*, *slc22a23*, *foxp4*, *nr2f6*, and *six3* in 48 hpf *kmt2d-/-* mutant zebrafish. Likewise, we performed qRT-PCR for *id3*, *prdm1a*, and *anxa4* in 48 hpf *kdm6a-/-* mutant zebrafish. Our results show decreased expression for *sox12*, *foxp4*, *nr2f6*, and *six3* in the *kmt2d-/-* mutant (Figure 4C), and *id3*, *prdm1a*, and *anxa4* in the *kdm6a-/-* mutant (Figure 5D).

Genes common to *KMT2D* datasets	**Table 1: Characteristics relevant to cardiac and overall development**
SOX12	Expressed mice outflow tract 12.5-16.5 dpc (days post coitum),

	Sox4$^{+/-}$*11*$^{+/-}$*12*$^{-/-}$ mice have common trunk or truncus arteriosus, a CHD with single outflow tract (Bhattaram et al., 2010; Hoser et al., 2008; Paul, Harvey, Wegner, & Sock, 2014), expressed broadly throughout neural plate and migrating NCCs (Uy, Simoes-Costa, Koo, Sauka-Spengler, & Bronner, 2015)
SLC22A23	Expressed in heart and integral to mouse heart development expressed in heart, integral in mouse heart developent (Aberg et al., 2012; Christoforou et al., 2008; Ekizoglu, Seven, Ulutin, Guliyev, & Buyru, 2018)
FOXP4	Mutants develop two hearts having proper chamber formation, and normal trabecular and compact myocardial development, with same heart rate but asynchronous, lethal at E12.5 (Li, Zhou, Lu, & Morrisey, 2004; Y. Zhang et al., 2010)
NR2F6	Important for normal cardiac morphogenesis, including the development of coronary vasculature, left ventricular compact zone, and heart valves PMID: (Crispino et al., 2001; Hermann-Kleiter & Baier, 2014; Huggins, Bacani, Boltax, Aikawa, & Leiden, 2001)
SIX3	Early brain development (Inbal, Kim, Shin, & Solnica-Krezel, 2007), mutation implicated in holoprosencephaly, coloboma, cleft lip/palate (Lacbawan et al., 2009)

434

Genes common to *KDM6A* datasets	**Table 2: Characteristics relevant to cardiac and overall development**
ID3	Knockout in various combinations with *ID1/2/4* causes ventricular septation defects, outflow tract atresia, missing heart tube-forming region, decreased heart size and function (Y. Chen et al., 2004; Cunningham et al., 2017; Fraidenraich et al., 2004; Hu, Xin, Hu, Sun, & Zhao, 2019)
PRDM1	Functions in mesoderm of second heart field, where it interacts with Tbx1, during outflow tract morphogenesis in mouse embryo (Vincent et al., 2014))

ANXA4	Expressed in cardiac myocytes and upregulated in human failing hearts (Lewin et al., 2009; Matteo & Moravec, 2000)

Our qRT-PCR results for *kmt2d-/-* mutant zebrafish show a downregulation of *sox12*, *foxp4*, *nr2f6*, and *six3*, thus displaying greater consistency with the zebrafish RNA seq where these genes are downregulated (Figure 4C). *Sox12*, *Foxp4*, and *Six3* are not downregulated, rather upregulated in varying degrees, in the mice RNA-seq (Figure 4C). *SOX12*, *FOXP4*, and *NR2F6* are not downregulated, rather upregulated in varying degrees, in the human RNA-seq (Figure 4C). Expression of *slc22a23* is not significantly changed in the qRT-PCR, though it is moderately upregulated in the zebrafish and mice RNA-seq, and highly in the human RNA seq (Figure 4C). The *KMT2D* and *KDM6A* datasets show variations in the expression patterns of same genes across different species and cell types which indicate a tight spatial and temporal orchestration of the roles of *KMT2D* and *KDM6A* in gene regulation.

The qRT-PCR results for the *kdm6a-/-* mutant zebrafish, show reduction in *id3*, *prdm1a*, and *anxa4* (Figure 5C), which are consistent with RNA-seq datasets from mouse NCCs and neural stem cells (Figure 5B). Additionally, *Prdm1* from mouse CD4+ RNA-seq, and *ANXA4* from human RNA seq, are downregulated as in the qRT-PCR data. The upregulation of *Id3* and *Anxa4* in RNA seq of mouse CD4+ cells, and *ID3* and *PRDM1* in RNA seq of humans may be attributed to differences in source cell types used, and differences in species-specific temporal and spatial regulation of gene expression by KDM6A which is not fully understood. It is interesting to note the similarities and differences in transcriptomic profiles of similar types of cells i.e. human lymphoblastoid and murine CD4+, respectively.

Discussion

Cardiac development is orchestrated by progenitor cells from the cardiogenic mesoderm, proepicardium, and cardiac neural crest cells (Brade et al., 2013). The mesoderm contributes to cardiac crescent and linear heart tube, the proepicardium contributes to chamber maturation and coronary vessel formation, and the cardiac neural crest cells contribute to outflow tract septation, aortic arch patterning, semilunar valves, cardiomyocytes in amniotes, and heart regeneration in

zebrafish (Brade et al., 2013; Jain et al., 2011; Tang, Martik, Li, & Bronner, 2019). Consequently, CHDs arise from disruption of cardiac progenitor cell development which is tightly orchestrated in a temporal and spatial manner by a complex network of genetic and epigenetic factors. Single cell-based high throughput assays further corroborate the transcriptional regulation of cardiogenesis (de Soysa et al., 2019). Epigenetic factors like *KMT2D* and *KDM6A* have been studied by several groups to identify how their mutations lead to heart defects. *KMT2D* and *KDM6A* are associated with crucial histone modifications - H3K4me3 and H3K27me3, respectively - which are linked to various aspects of cardiac development and disease.

Here we present, for the first time, a comparison between the transcriptome of zebrafish, mice, and humans with mutations in *KMT2D*, and a comparison between transcriptomes of humans and three distinct cell populations of mice with mutations in *KDM6A*. A subset of genes involved in cardiac development and physiology, vasculature, and overall development, appeared as common targets across all datasets for each mutation. Specifically, our analysis revealed 76 genes as common targets of *KMT2D* upon comparing our human datasets with the zebrafish and mouse datasets. 30 out of 76 genes show a similar expression pattern across the 3 species, while 46 genes do not. The dissimilar expression patterns of the 46 genes can partly be explained by the fact that the transcriptomes of the 3 species are derived from different cell populations derived during different stages of life. Hence, epigenetic regulation by KMT2D is tightly orchestrated spatially and temporally. On the other hand, a similar expression pattern in 3 species for the 30 genes by KMT2D indicates that its role is partly conserved. For *KDM6A*, we identified 7 common targets upon comparing human RNA-seq datasets with 3 mice datasets obtained from neural crest, neural stem, and CD4+ cells. Our *in vivo* analysis of *kmt2d* and *kdm6a* mutations in zebrafish corroborate the findings of previous studies investigating these two genes in cardiac development and disease (Ang et al., 2016; Lee et al., 2012; Schwenty-Lara, Nurnberger, et al., 2019; Serrano et al., 2019).

Serrano et al. have shown that *kmt2d* mutations in zebrafish cause defects in cardiovascular development, angiogenesis and aortic arch formation, as well as cardiac hypoplasticity (Serrano et al., 2019). Kmt2d associates with genes in cardiomyocytes, and myocardial deletion of *Kmt2d* reduces cardiac gene expression during murine heart development

(Ang et al., 2016). In *xenopus*, morpholino-based knockdown of *kmt2d* causes cardiac hypoplasticity, reduced expression of early cardiac developmental genes like *tbx20*, *isl1*, *nkx2.5* (Schwenty-Lara, Nurnberger, et al., 2019), and impaired formation and migration of NCCs by reducing the expression of early NCC-specific markers like *pax3*, *foxd3*, *twist*, and *slug* (Schwenty-Lara, Nehl, et al., 2019).

On the other hand, *KDM6A* or *Utx* promotes the differentiation of mouse embryonic stem cells (ESCs) into a cardiac lineage, and serves as a co-activator of core cardiac transcription factors like *Srf, Nkx2.5*, *Tbx5*, and *Gata4* (Lee et al., 2012). *KDM6A* or *Utx* associates with cardiac-specific genes like *Anf* and *Baf60c*, to help recruit Brg1, an ATP-dependent chromatin remodeler that activates transcription of core cardiac transcription factors (Hang et al., 2010; Lee et al., 2012; Lickert et al., 2004). A neural crest-specific conditional deletion of *KDM6A* or *Utx* allele with a *Wnt1-Cre* transgene causes CHDs like patent ductus arteriosus (Shpargel et al., 2017).

While we observe a modest reduction in the early specification of NCCs (*sox10* and *foxd3*, Figure 3) in zebrafish mutants of *kmt2d* and *kdm6a*, migration appears normal for the most part since we do not see drastic reduction of the number of cells in the developing heart (Figures 2 and 3). Likewise, our *in vivo* analysis of zebrafish shows a decrease in expression of NCCs-specific markers of early cardiac development like *hand2a* and *mef2ca* (Figure 2). Together, our study underscores several recent publications on the roles of *KMT2D* and *KDM6A* during early developmental stages of the heart and cardiac NCCs. Our cross-species transcriptomic analysis reveals conserved and unique gene expression patterns for *KMT2D* and *KDM6A*.

Our work on *KMT2D* and *KDM6A* can potentially contribute to future studies on cardiac regeneration, reprogramming, and disease where H3K4me3 and H3K27me3 are implicated (Ben-Yair et al., 2019; Delgado-Olguin et al., 2012; Engel & Ardehali, 2018; He et al., 2012; Ieda et al., 2010; Jonsson et al., 2016; Kaneda et al., 2009; Lee et al., 2012; C. F. Liu & Tang, 2019; L. Liu, I. Lei, H. Karatas, et al., 2016; L. Liu, Lei, & Wang, 2016; Z. Liu et al., 2016; Mathiyalagan, Keating, Du, & El-Osta, 2014; Monroe et al., 2019; Papait et al., 2013; Rosa-Garrido, Chapski, & Vondriska, 2018; Stein et al., 2011; Q. J. Zhang & Liu, 2015). In zebrafish, H3K27me3 has recently been shown to silence structural genes in proliferating cardiomyocytes during wound invasion and regeneration of injured hearts (Ben-Yair et al., 2019). ChIP-

sequencing studies on primary neonatal murine cardiomyocytes revealed that H3K4me3 is enriched, while H3K27me3 is reduced, at promoters of cardiac-specific genes like *Mef2c*, *Gata4*, and *Tbx5* (Z. Liu et al., 2016). This study further showed that early re-patterning of H3K4me3 and H3K27me3 occurs during reprogramming of induced cardiomyocytes (iCMs), which are used for modeling cardiac diseases and regeneration (Z. Liu et al., 2016).

A study on the integration of ChIP- and ATAC-sequencing of adult and fetal human cardiac fibroblasts (HCFs) revealed that open chromatin or ATAC-seq peaks overlaid active promoters marked by H3K4me3 but not the repressive mark of H3K27me3 (Jonsson et al., 2016). However, both H3K4me3 and H3M27me3 were enriched around transcriptional start sites of their corresponding target genes (Jonsson et al., 2016). Moreover, ChIP-sequencing of adult murine cardiomyocytes followed by Gene Ontology (GO) analysis with the Genomic Regions Enrichment of Annotations Tool (GREAT) revealed that sites with differential distribution of H3K4me3 and H3K27me3 are associated with hypertrophic murine heart phenotypes, like thick ventricular wall, altered heart contraction, impaired skeletal muscle contractility, and abnormal cardiac stroke volume (Papait et al., 2013). During embryogenesis, enrichment of germ layer-specific H3K27me3 has been identified at sites of high DNA methylation in undifferentiated states (Gifford et al., 2013). Hence, the complexities of epigenetic modifications associated with *KMT2D* and *KDM6A* in cardiac biology are gradually being understood.

Mutations in *KMT2D* and *KDM6A* also contribute to complications during pregnancy (Rosenberg et al., 2020). Polyhydramnios or excessive amniotic fluid in the amniotic sac, reduced placental weights, and abnormal quadruple marker tests are reported from an analysis of 49 individuals with KS and their mothers (Rosenberg et al., 2020). Building on clinical data, (Adam et al., 2019; Adam, Hudgins, & Hannibal, 1993; Y. R. Wang, Xu, Wang, & Wang, 2019), interventions via genetic counselling and ongoing research on small molecule-based epigenetic inhibitors can provide potential diagnostic and preventive solutions for Kabuki Syndrome-based obstetric disorders.

Interestingly, missense *KMT2D* variants have also been correlated with a novel multiple malformations syndrome that is distinct from KS (Cuvertino et al., 2020), while *KDM6A* mutations are implicated in autoimmunity and drug resistance in leukemia (Itoh et al., 2019; Stief et al., 2020). Frequent immunopathological manifestations like immune thrombocytopenic

purpura, vitiligo, etc. have also been reported from a registry study on 177 individuals with mutations in *KMT2D* or *KDM6A* (Margot et al., 2020).

To conclude, several features of the roles of *KMT2D* and *KDM6A* remain to be deciphered, especially other factors which cross-talk with H3K4me3/K27me3 and are linked to CHDs like *KDM1A*/*LSD1*, *KDM4A*, *KDM4C*, *EZH2*, and cilia (Agger et al., 2007; Ahmed & Streit, 2018; L. Chen et al., 2012; Lee et al., 2012; Nicholson et al., 2013; Rosales, Carulla, Garcia, Vargas, & Lizcano, 2016; Willaredt, Gorgas, Gardner, & Tucker, 2012; Wu et al., 2015; Y. Yang et al., 2019; Q. J. Zhang et al., 2011). FDA-approved drugs targeting inhibitors of LSD1 and EZH2 are used in treating cancers, which provide hope for expansion towards developing epigenetics-based therapies against heart disease. Interestingly, *KMT2D* and *KDM6A* mutations are also implicated in cancers (Kantidakis et al., 2016; L. Wang & Shilatifard, 2019), and cardiotoxicity is reported as a side-effect in some but not all patients who receive cancer therapies which has evolved to a new field of study called cardio-oncology. Although at a nascent stage, the links between epigenetic factors in cardiac development and health, and cancers, can potentially address important questions in cardio-oncology. Taken together, a comprehensive understanding of epigenetic regulation of heart development and disease, in combination with large next-generation sequencing datasets from patients that are continuously being generated, combined with animal models can contribute to the emerging field of personalized medicine to translate epigenetics-based research from the bench to the bedside.

Acknowledgements

We acknowledge Maria de los Angeles Serrano and H. Joseph Yost for providing the complete dataset of *kmt2d* mutant zebrafish RNA sequencing as referenced in (Serrano et al., 2019). The study was supported by Summer 2018 Postdoctoral Fellowship to R. Sen from the American Heart Association (18POST33960371), funding from Dr. K.B. Artinger (R01DE024034). E.L is supported by a National Institutes of Health Ruth L. Kirschstein National Research Service Award T32 Postdoctoral Fellowship (T32CA17468).

Conflicts of Interest

The authors declare no conflicts of interest

582 Aberg, K., Adkins, D. E., Liu, Y., McClay, J. L., Bukszar, J., Jia, P., . . . van den Oord, E. J. (2012). Genome-
583 wide association study of antipsychotic-induced QTc interval prolongation. *Pharmacogenomics*
584 *J, 12*(2), 165-172. doi:10.1038/tpj.2010.76
585 Accari, S. L., & Fisher, P. R. (2015). Emerging Roles of JmjC Domain-Containing Proteins. *Int Rev Cell Mol*
586 *Biol, 319*, 165-220. doi:10.1016/bs.ircmb.2015.07.003
587 Adam, M. P., Banka, S., Bjornsson, H. T., Bodamer, O., Chudley, A. E., Harris, J., . . . Kabuki Syndrome
588 Medical Advisory, B. (2019). Kabuki syndrome: international consensus diagnostic criteria. *J Med*
589 *Genet, 56*(2), 89-95. doi:10.1136/jmedgenet-2018-105625
590 Adam, M. P., Hudgins, L., & Hannibal, M. (1993). Kabuki Syndrome. In M. P. Adam, H. H. Ardinger, R. A.
591 Pagon, S. E. Wallace, L. J. H. Bean, K. Stephens, & A. Amemiya (Eds.), *GeneReviews((R))*. Seattle
592 (WA).
593 Agger, K., Cloos, P. A., Christensen, J., Pasini, D., Rose, S., Rappsilber, J., . . . Helin, K. (2007). UTX and
594 JMJD3 are histone H3K27 demethylases involved in HOX gene regulation and development.
595 *Nature, 449*(7163), 731-734. doi:10.1038/nature06145
596 Ahmed, M., & Streit, A. (2018). Lsd1 interacts with cMyb to demethylate repressive histone marks and
597 maintain inner ear progenitor identity. *Development, 145*(4). doi:10.1242/dev.160325
598 Akerberg, A. A., Henner, A., Stewart, S., & Stankunas, K. (2017). Histone demethylases Kdm6ba and
599 Kdm6bb redundantly promote cardiomyocyte proliferation during zebrafish heart ventricle
600 maturation. *Dev Biol, 426*(1), 84-96. doi:10.1016/j.ydbio.2017.03.030
601 Ali, M., Hom, R. A., Blakeslee, W., Ikenouye, L., & Kutateladze, T. G. (2014). Diverse functions of PHD
602 fingers of the MLL/KMT2 subfamily. *Biochim Biophys Acta, 1843*(2), 366-371.
603 doi:10.1016/j.bbamcr.2013.11.016
604 Ang, S. Y., Uebersohn, A., Spencer, C. I., Huang, Y., Lee, J. E., Ge, K., & Bruneau, B. G. (2016). KMT2D
605 regulates specific programs in heart development via histone H3 lysine 4 di-methylation.
606 *Development, 143*(5), 810-821. doi:10.1242/dev.132688
607 Aoki, Y., Saint-Germain, N., Gyda, M., Magner-Fink, E., Lee, Y. H., Credidio, C., & Saint-Jeannet, J. P.
608 (2003). Sox10 regulates the development of neural crest-derived melanocytes in Xenopus. *Dev*
609 *Biol, 259*(1), 19-33. doi:10.1016/s0012-1606(03)00161-1
610 Ben-Yair, R., Butty, V. L., Busby, M., Qiu, Y., Levine, S. S., Goren, A., . . . Burns, C. E. (2019). H3K27me3-
611 mediated silencing of structural genes is required for zebrafish heart regeneration.
612 *Development, 146*(19). doi:10.1242/dev.178632
613 Benjamin, E. J., Muntner, P., Alonso, A., Bittencourt, M. S., Callaway, C. W., Carson, A. P., . . . Stroke
614 Statistics, S. (2019). Heart Disease and Stroke Statistics-2019 Update: A Report From the
615 American Heart Association. *Circulation, 139*(10), e56-e528.
616 doi:10.1161/CIR.0000000000000659
617 Bhattaram, P., Penzo-Mendez, A., Sock, E., Colmenares, C., Kaneko, K. J., Vassilev, A., . . . Lefebvre, V.
618 (2010). Organogenesis relies on SoxC transcription factors for the survival of neural and
619 mesenchymal progenitors. *Nat Commun, 1*, 9. doi:10.1038/ncomms1008
620 Brade, T., Pane, L. S., Moretti, A., Chien, K. R., & Laugwitz, K. L. (2013). Embryonic heart progenitors and
621 cardiogenesis. *Cold Spring Harb Perspect Med, 3*(10), a013847.
622 doi:10.1101/cshperspect.a013847
623 Buckingham, M., Meilhac, S., & Zaffran, S. (2005). Building the mammalian heart from two sources of
624 myocardial cells. *Nat Rev Genet, 6*(11), 826-835. doi:10.1038/nrg1710
625 Campeau, P. M., Lu, J. T., Dawson, B. C., Fokkema, I. F., Robertson, S. P., Gibbs, R. A., & Lee, B. H. (2012).
626 The KAT6B-related disorders genitopatellar syndrome and Ohdo/SBBYS syndrome have distinct
627 clinical features reflecting distinct molecular mechanisms. *Hum Mutat, 33*(11), 1520-1525.
628 doi:10.1002/humu.22141

629 Chen, L., Ma, Y., Kim, E. Y., Yu, W., Schwartz, R. J., Qian, L., & Wang, J. (2012). Conditional ablation of
630 Ezh2 in murine hearts reveals its essential roles in endocardial cushion formation,
631 cardiomyocyte proliferation and survival. *PLoS One, 7*(2), e31005.
632 doi:10.1371/journal.pone.0031005
633 Chen, Y., Mironova, E., Whitaker, L. L., Edwards, L., Yost, H. J., & Ramsdell, A. F. (2004). ALK4 functions as
634 a receptor for multiple TGF beta-related ligands to regulate left-right axis determination and
635 mesoderm induction in Xenopus. *Dev Biol, 268*(2), 280-294. doi:10.1016/j.ydbio.2003.12.035
636 Christoforou, N., Miller, R. A., Hill, C. M., Jie, C. C., McCallion, A. S., & Gearhart, J. D. (2008). Mouse ES
637 cell-derived cardiac precursor cells are multipotent and facilitate identification of novel cardiac
638 genes. *J Clin Invest, 118*(3), 894-903. doi:10.1172/JCI33942
639 Cocciadiferro, D., Augello, B., De Nittis, P., Zhang, J., Mandriani, B., Malerba, N., . . . Merla, G. (2018).
640 Dissecting KMT2D missense mutations in Kabuki syndrome patients. *Hum Mol Genet, 27*(21),
641 3651-3668. doi:10.1093/hmg/ddy241
642 Crispino, J. D., Lodish, M. B., Thurberg, B. L., Litovsky, S. H., Collins, T., Molkentin, J. D., & Orkin, S. H.
643 (2001). Proper coronary vascular development and heart morphogenesis depend on interaction
644 of GATA-4 with FOG cofactors. *Genes Dev, 15*(7), 839-844. doi:10.1101/gad.875201
645 Crump, N. T., & Milne, T. A. (2019). Why are so many MLL lysine methyltransferases required for normal
646 mammalian development? *Cell Mol Life Sci, 76*(15), 2885-2898. doi:10.1007/s00018-019-03143-
647 z
648 Cunningham, T. J., Yu, M. S., McKeithan, W. L., Spiering, S., Carrette, F., Huang, C. T., . . . Colas, A. R.
649 (2017). Id genes are essential for early heart formation. *Genes Dev, 31*(13), 1325-1338.
650 doi:10.1101/gad.300400.117
651 Cuvertino, S., Hartill, V., Colyer, A., Garner, T., Nair, N., Al-Gazali, L., . . . Banka, S. (2020). A restricted
652 spectrum of missense KMT2D variants cause a multiple malformations disorder distinct from
653 Kabuki syndrome. *Genet Med*. doi:10.1038/s41436-019-0743-3
654 de Soysa, T. Y., Ranade, S. S., Okawa, S., Ravichandran, S., Huang, Y., Salunga, H. T., . . . Srivastava, D.
655 (2019). Single-cell analysis of cardiogenesis reveals basis for organ-level developmental defects.
656 *Nature, 572*(7767), 120-124. doi:10.1038/s41586-019-1414-x
657 Delgado-Olguin, P., Huang, Y., Li, X., Christodoulou, D., Seidman, C. E., Seidman, J. G., . . . Bruneau, B. G.
658 (2012). Epigenetic repression of cardiac progenitor gene expression by Ezh2 is required for
659 postnatal cardiac homeostasis. *Nat Genet, 44*(3), 343-347. doi:10.1038/ng.1068
660 Digilio, M. C., Gnazzo, M., Lepri, F., Dentici, M. L., Pisaneschi, E., Baban, A., . . . Dallapiccola, B. (2017).
661 Congenital heart defects in molecularly proven Kabuki syndrome patients. *Am J Med Genet A,*
662 *173*(11), 2912-2922. doi:10.1002/ajmg.a.38417
663 Dobin, A., Davis, C. A., Schlesinger, F., Drenkow, J., Zaleski, C., Jha, S., . . . Gingeras, T. R. (2013). STAR:
664 ultrafast universal RNA-seq aligner. *Bioinformatics, 29*(1), 15-21.
665 doi:10.1093/bioinformatics/bts635
666 Dutton, K. A., Pauliny, A., Lopes, S. S., Elworthy, S., Carney, T. J., Rauch, J., . . . Kelsh, R. N. (2001).
667 Zebrafish colourless encodes sox10 and specifies non-ectomesenchymal neural crest fates.
668 *Development, 128*(21), 4113-4125.
669 Ekizoglu, S., Seven, D., Ulutin, T., Guliyev, J., & Buyru, N. (2018). Investigation of the SLC22A23 gene in
670 laryngeal squamous cell carcinoma. *BMC Cancer, 18*(1), 477. doi:10.1186/s12885-018-4381-y
671 Engel, J. L., & Ardehali, R. (2018). Direct Cardiac Reprogramming: Progress and Promise. *Stem Cells Int,*
672 *2018*, 1435746. doi:10.1155/2018/1435746
673 Fahrner, J. A., Lin, W. Y., Riddle, R. C., Boukas, L., DeLeon, V. B., Chopra, S., . . . Bjornsson, H. T. (2019).
674 Precocious chondrocyte differentiation disrupts skeletal growth in Kabuki syndrome mice. *JCI*
675 *Insight, 4*(20). doi:10.1172/jci.insight.129380

Faralli, H., Wang, C., Nakka, K., Benyoucef, A., Sebastian, S., Zhuang, L., . . . Dilworth, F. J. (2016). UTX demethylase activity is required for satellite cell-mediated muscle regeneration. *J Clin Invest, 126*(4), 1555-1565. doi:10.1172/JCI83239

Fellous, A., Earley, R. L., & Silvestre, F. (2019). The Kdm/Kmt gene families in the self-fertilizing mangrove rivulus fish, Kryptolebias marmoratus, suggest involvement of histone methylation machinery in development and reproduction. *Gene, 687*, 173-187. doi:10.1016/j.gene.2018.11.046

Fraidenraich, D., Stillwell, E., Romero, E., Wilkes, D., Manova, K., Basson, C. T., & Benezra, R. (2004). Rescue of cardiac defects in id knockout embryos by injection of embryonic stem cells. *Science, 306*(5694), 247-252. doi:10.1126/science.1102612

Gagnon, J. A., Valen, E., Thyme, S. B., Huang, P., Akhmetova, L., Pauli, A., . . . Schier, A. F. (2014). Efficient mutagenesis by Cas9 protein-mediated oligonucleotide insertion and large-scale assessment of single-guide RNAs. *PLoS One, 9*(5), e98186. doi:10.1371/journal.pone.0098186

Gazova, I., Lengeling, A., & Summers, K. M. (2019). Lysine demethylases KDM6A and UTY: The X and Y of histone demethylation. *Mol Genet Metab, 127*(1), 31-44. doi:10.1016/j.ymgme.2019.04.012

George, V., Colombo, S., & Targoff, K. L. (2015). An early requirement for nkx2.5 ensures the first and second heart field ventricular identity and cardiac function into adulthood. *Dev Biol, 400*(1), 10-22. doi:10.1016/j.ydbio.2014.12.019

Gifford, C. A., Ziller, M. J., Gu, H., Trapnell, C., Donaghey, J., Tsankov, A., . . . Meissner, A. (2013). Transcriptional and epigenetic dynamics during specification of human embryonic stem cells. *Cell, 153*(5), 1149-1163. doi:10.1016/j.cell.2013.04.037

Gilboa, S. M., Salemi, J. L., Nembhard, W. N., Fixler, D. E., & Correa, A. (2010). Mortality resulting from congenital heart disease among children and adults in the United States, 1999 to 2006. *Circulation, 122*(22), 2254-2263. doi:10.1161/CIRCULATIONAHA.110.947002

Hang, C. T., Yang, J., Han, P., Cheng, H. L., Shang, C., Ashley, E., . . . Chang, C. P. (2010). Chromatin regulation by Brg1 underlies heart muscle development and disease. *Nature, 466*(7302), 62-67. doi:10.1038/nature09130

He, A., Ma, Q., Cao, J., von Gise, A., Zhou, P., Xie, H., . . . Pu, W. T. (2012). Polycomb repressive complex 2 regulates normal development of the mouse heart. *Circ Res, 110*(3), 406-415. doi:10.1161/CIRCRESAHA.111.252205

Hermann-Kleiter, N., & Baier, G. (2014). Orphan nuclear receptor NR2F6 acts as an essential gatekeeper of Th17 CD4+ T cell effector functions. *Cell Commun Signal, 12*, 38. doi:10.1186/1478-811X-12-38

Herrmann, F., Gross, A., Zhou, D., Kestler, H. A., & Kuhl, M. (2012). A boolean model of the cardiac gene regulatory network determining first and second heart field identity. *PLoS One, 7*(10), e46798. doi:10.1371/journal.pone.0046798

Hinits, Y., Pan, L., Walker, C., Dowd, J., Moens, C. B., & Hughes, S. M. (2012). Zebrafish Mef2ca and Mef2cb are essential for both first and second heart field cardiomyocyte differentiation. *Dev Biol, 369*(2), 199-210. doi:10.1016/j.ydbio.2012.06.019

Hong, S., Cho, Y. W., Yu, L. R., Yu, H., Veenstra, T. D., & Ge, K. (2007). Identification of JmjC domain-containing UTX and JMJD3 as histone H3 lysine 27 demethylases. *Proc Natl Acad Sci U S A, 104*(47), 18439-18444. doi:10.1073/pnas.0707292104

Hoser, M., Potzner, M. R., Koch, J. M., Bosl, M. R., Wegner, M., & Sock, E. (2008). Sox12 deletion in the mouse reveals nonreciprocal redundancy with the related Sox4 and Sox11 transcription factors. *Mol Cell Biol, 28*(15), 4675-4687. doi:10.1128/MCB.00338-08

Hu, W., Xin, Y., Hu, J., Sun, Y., & Zhao, Y. (2019). Inhibitor of DNA binding in heart development and cardiovascular diseases. *Cell Commun Signal, 17*(1), 51. doi:10.1186/s12964-019-0365-z

722 Huang, C. J., Tu, C. T., Hsiao, C. D., Hsieh, F. J., & Tsai, H. J. (2003). Germ-line transmission of a
723 myocardium-specific GFP transgene reveals critical regulatory elements in the cardiac myosin
724 light chain 2 promoter of zebrafish. *Dev Dyn, 228*(1), 30-40. doi:10.1002/dvdy.10356
725 Huggins, G. S., Bacani, C. J., Boltax, J., Aikawa, R., & Leiden, J. M. (2001). Friend of GATA 2 physically
726 interacts with chicken ovalbumin upstream promoter-TF2 (COUP-TF2) and COUP-TF3 and
727 represses COUP-TF2-dependent activation of the atrial natriuretic factor promoter. *J Biol Chem,*
728 *276*(30), 28029-28036. doi:10.1074/jbc.M103577200
729 Ieda, M., Fu, J. D., Delgado-Olguin, P., Vedantham, V., Hayashi, Y., Bruneau, B. G., & Srivastava, D.
730 (2010). Direct reprogramming of fibroblasts into functional cardiomyocytes by defined factors.
731 *Cell, 142*(3), 375-386. doi:10.1016/j.cell.2010.07.002
732 Inbal, A., Kim, S. H., Shin, J., & Solnica-Krezel, L. (2007). Six3 represses nodal activity to establish early
733 brain asymmetry in zebrafish. *Neuron, 55*(3), 407-415. doi:10.1016/j.neuron.2007.06.037
734 Itoh, Y., Golden, L. C., Itoh, N., Matsukawa, M. A., Ren, E., Tse, V., . . . Voskuhl, R. R. (2019). The X-linked
735 histone demethylase Kdm6a in CD4+ T lymphocytes modulates autoimmunity. *J Clin Invest, 130*,
736 3852-3863. doi:10.1172/JCI126250
737 Jain, R., Engleka, K. A., Rentschler, S. L., Manderfield, L. J., Li, L., Yuan, L., & Epstein, J. A. (2011). Cardiac
738 neural crest orchestrates remodeling and functional maturation of mouse semilunar valves. *J*
739 *Clin Invest, 121*(1), 422-430. doi:10.1172/JCI44244
740 Jonsson, M. K. B., Hartman, R. J. G., Ackers-Johnson, M., Tan, W. L. W., Lim, B., van Veen, T. A. B., & Foo,
741 R. S. (2016). A Transcriptomic and Epigenomic Comparison of Fetal and Adult Human Cardiac
742 Fibroblasts Reveals Novel Key Transcription Factors in Adult Cardiac Fibroblasts. *JACC Basic*
743 *Transl Sci, 1*(7), 590-602. doi:10.1016/j.jacbts.2016.07.007
744 Kaneda, R., Takada, S., Yamashita, Y., Choi, Y. L., Nonaka-Sarukawa, M., Soda, M., . . . Mano, H. (2009).
745 Genome-wide histone methylation profile for heart failure. *Genes Cells, 14*(1), 69-77.
746 doi:10.1111/j.1365-2443.2008.01252.x
747 Kantidakis, T., Saponaro, M., Mitter, R., Horswell, S., Kranz, A., Boeing, S., . . . Svejstrup, J. Q. (2016).
748 Mutation of cancer driver MLL2 results in transcription stress and genome instability. *Genes Dev,*
749 *30*(4), 408-420. doi:10.1101/gad.275453.115
750 Kimmel, C. B., Ballard, W. W., Kimmel, S. R., Ullmann, B., & Schilling, T. F. (1995). Stages of embryonic
751 development of the zebrafish. *Dev Dyn, 203*(3), 253-310. doi:10.1002/aja.1002030302
752 Klose, R. J., Kallin, E. M., & Zhang, Y. (2006). JmjC-domain-containing proteins and histone
753 demethylation. *Nat Rev Genet, 7*(9), 715-727. doi:10.1038/nrg1945
754 Koutsioumpa, M., Hatziapostolou, M., Polytarchou, C., Tolosa, E. J., Almada, L. L., Mahurkar-Joshi, S., . . .
755 Iliopoulos, D. (2019). Lysine methyltransferase 2D regulates pancreatic carcinogenesis through
756 metabolic reprogramming. *Gut, 68*(7), 1271-1286. doi:10.1136/gutjnl-2017-315690
757 Labosky, P. A., & Kaestner, K. H. (1998). The winged helix transcription factor Hfh2 is expressed in neural
758 crest and spinal cord during mouse development. *Mech Dev, 76*(1-2), 185-190.
759 doi:10.1016/s0925-4773(98)00105-1
760 Lacbawan, F., Solomon, B. D., Roessler, E., El-Jaick, K., Domene, S., Velez, J. I., . . . Muenke, M. (2009).
761 Clinical spectrum of SIX3-associated mutations in holoprosencephaly: correlation between
762 genotype, phenotype and function. *J Med Genet, 46*(6), 389-398. doi:10.1136/jmg.2008.063818
763 Lan, F., Bayliss, P. E., Rinn, J. L., Whetstine, J. R., Wang, J. K., Chen, S., . . . Shi, Y. (2007). A histone H3
764 lysine 27 demethylase regulates animal posterior development. *Nature, 449*(7163), 689-694.
765 doi:10.1038/nature06192
766 Laugwitz, K. L., Moretti, A., Caron, L., Nakano, A., & Chien, K. R. (2008). Islet1 cardiovascular progenitors:
767 a single source for heart lineages? *Development, 135*(2), 193-205. doi:10.1242/dev.001883

768 Lee, S., Lee, J. W., & Lee, S. K. (2012). UTX, a histone H3-lysine 27 demethylase, acts as a critical switch to
769 activate the cardiac developmental program. *Dev Cell, 22*(1), 25-37.
770 doi:10.1016/j.devcel.2011.11.009
771 Lei, X., & Jiao, J. (2018). UTX Affects Neural Stem Cell Proliferation and Differentiation through PTEN
772 Signaling. *Stem Cell Reports, 10*(4), 1193-1207. doi:10.1016/j.stemcr.2018.02.008
773 Lewin, G., Matus, M., Basu, A., Frebel, K., Rohsbach, S. P., Safronenko, A., . . . Muller, F. U. (2009). Critical
774 role of transcription factor cyclic AMP response element modulator in beta1-adrenoceptor-
775 mediated cardiac dysfunction. *Circulation, 119*(1), 79-88.
776 doi:10.1161/CIRCULATIONAHA.108.786533
777 Li, S., Zhou, D., Lu, M. M., & Morrisey, E. E. (2004). Advanced cardiac morphogenesis does not require
778 heart tube fusion. *Science, 305*(5690), 1619-1622. doi:10.1126/science.1098674
779 Lickert, H., Takeuchi, J. K., Von Both, I., Walls, J. R., McAuliffe, F., Adamson, S. L., . . . Bruneau, B. G.
780 (2004). Baf60c is essential for function of BAF chromatin remodelling complexes in heart
781 development. *Nature, 432*(7013), 107-112. doi:10.1038/nature03071
782 Liu, C. F., & Tang, W. H. W. (2019). Epigenetics in Cardiac Hypertrophy and Heart Failure. *JACC Basic*
783 *Transl Sci, 4*(8), 976-993. doi:10.1016/j.jacbts.2019.05.011
784 Liu, L., Lei, I., Karatas, H., Li, Y., Wang, L., Gnatovskiy, L., . . . Wang, Z. (2016). Targeting Mll1 H3K4
785 methyltransferase activity to guide cardiac lineage specific reprogramming of fibroblasts. *Cell*
786 *Discov, 2*, 16036. doi:10.1038/celldisc.2016.36
787 Liu, L., Lei, I., & Wang, Z. (2016). Improving cardiac reprogramming for heart regeneration. *Curr Opin*
788 *Organ Transplant, 21*(6), 588-594. doi:10.1097/MOT.0000000000000363
789 Liu, Z., Chen, O., Zheng, M., Wang, L., Zhou, Y., Yin, C., . . . Qian, L. (2016). Re-patterning of H3K27me3,
790 H3K4me3 and DNA methylation during fibroblast conversion into induced cardiomyocytes. *Stem*
791 *Cell Res, 16*(2), 507-518. doi:10.1016/j.scr.2016.02.037
792 Love, M. I., Huber, W., & Anders, S. (2014). Moderated estimation of fold change and dispersion for
793 RNA-seq data with DESeq2. *Genome Biol, 15*(12), 550. doi:10.1186/s13059-014-0550-8
794 Lu, F., Langenbacher, A. D., & Chen, J. N. (2016). Transcriptional Regulation of Heart Development in
795 Zebrafish. *J Cardiovasc Dev Dis, 3*(2). doi:10.3390/jcdd3020014
796 Luo, R., An, M., Arduini, B. L., & Henion, P. D. (2001). Specific pan-neural crest expression of zebrafish
797 Crestin throughout embryonic development. *Dev Dyn, 220*(2), 169-174. doi:10.1002/1097-
798 0177(2000)9999:9999<::AID-DVDY1097>3.0.CO;2-1
799 Luperchio, T. R., Applegate, C. D., Bodamer, O., & Bjornsson, H. T. (2019). Haploinsufficiency of KMT2D is
800 sufficient to cause Kabuki syndrome and is compatible with life. *Mol Genet Genomic Med*,
801 e1072. doi:10.1002/mgg3.1072
802 Margot, H., Boursier, G., Duflos, C., Sanchez, E., Amiel, J., Andrau, J. C., . . . Genevieve, D. (2020).
803 Immunopathological manifestations in Kabuki syndrome: a registry study of 177 individuals.
804 *Genet Med, 22*(1), 181-188. doi:10.1038/s41436-019-0623-x
805 Mathiyalagan, P., Keating, S. T., Du, X. J., & El-Osta, A. (2014). Chromatin modifications remodel cardiac
806 gene expression. *Cardiovasc Res, 103*(1), 7-16. doi:10.1093/cvr/cvu122
807 Matteo, R. G., & Moravec, C. S. (2000). Immunolocalization of annexins IV, V and VI in the failing and
808 non-failing human heart. *Cardiovasc Res, 45*(4), 961-970. doi:10.1016/s0008-6363(99)00409-5
809 Maves, L., Tyler, A., Moens, C. B., & Tapscott, S. J. (2009). Pbx acts with Hand2 in early myocardial
810 differentiation. *Dev Biol, 333*(2), 409-418. doi:10.1016/j.ydbio.2009.07.004
811 McFadden, D. G., Barbosa, A. C., Richardson, J. A., Schneider, M. D., Srivastava, D., & Olson, E. N. (2005).
812 The Hand1 and Hand2 transcription factors regulate expansion of the embryonic cardiac
813 ventricles in a gene dosage-dependent manner. *Development, 132*(1), 189-201.
814 doi:10.1242/dev.01562

Monroe, T. O., Hill, M. C., Morikawa, Y., Leach, J. P., Heallen, T., Cao, S., . . . Martin, J. F. (2019). YAP Partially Reprograms Chromatin Accessibility to Directly Induce Adult Cardiogenesis In Vivo. *Dev Cell, 48*(6), 765-779 e767. doi:10.1016/j.devcel.2019.01.017

Moretti, A., Caron, L., Nakano, A., Lam, J. T., Bernshausen, A., Chen, Y., . . . Chien, K. R. (2006). Multipotent embryonic isl1+ progenitor cells lead to cardiac, smooth muscle, and endothelial cell diversification. *Cell, 127*(6), 1151-1165. doi:10.1016/j.cell.2006.10.029

Nicholson, T. B., Singh, A. K., Su, H., Hevi, S., Wang, J., Bajko, J., . . . Chen, T. (2013). A hypomorphic lsd1 allele results in heart development defects in mice. *PLoS One, 8*(4), e60913. doi:10.1371/journal.pone.0060913

Nottke, A., Colaiacovo, M. P., & Shi, Y. (2009). Developmental roles of the histone lysine demethylases. *Development, 136*(6), 879-889. doi:10.1242/dev.020966

Oster, M. E., Lee, K. A., Honein, M. A., Riehle-Colarusso, T., Shin, M., & Correa, A. (2013). Temporal trends in survival among infants with critical congenital heart defects. *Pediatrics, 131*(5), e1502-1508. doi:10.1542/peds.2012-3435

Ottaviani, G., & Buja, L. M. (2017). Update on congenital heart disease and sudden infant/perinatal death: from history to future trends. *J Clin Pathol, 70*(7), 555-562. doi:10.1136/jclinpath-2017-204326

Papait, R., Cattaneo, P., Kunderfranco, P., Greco, C., Carullo, P., Guffanti, A., . . . Condorelli, G. (2013). Genome-wide analysis of histone marks identifying an epigenetic signature of promoters and enhancers underlying cardiac hypertrophy. *Proc Natl Acad Sci U S A, 110*(50), 20164-20169. doi:10.1073/pnas.1315155110

Paul, M. H., Harvey, R. P., Wegner, M., & Sock, E. (2014). Cardiac outflow tract development relies on the complex function of Sox4 and Sox11 in multiple cell types. *Cell Mol Life Sci, 71*(15), 2931-2945. doi:10.1007/s00018-013-1523-x

Rosa-Garrido, M., Chapski, D. J., & Vondriska, T. M. (2018). Epigenomes in Cardiovascular Disease. *Circ Res, 122*(11), 1586-1607. doi:10.1161/CIRCRESAHA.118.311597

Rosales, W., Carulla, J., Garcia, J., Vargas, D., & Lizcano, F. (2016). Role of Histone Demethylases in Cardiomyocytes Induced to Hypertrophy. *Biomed Res Int, 2016*, 2634976. doi:10.1155/2016/2634976

Rosenberg, C. E., Daly, T., Hung, C., Hsueh, I., Lindsley, A. W., & Bodamer, O. (2020). Prenatal and perinatal history in Kabuki Syndrome. *Am J Med Genet A, 182*(1), 85-92. doi:10.1002/ajmg.a.61387

Rubinstein, A. L., Lee, D., Luo, R., Henion, P. D., & Halpern, M. E. (2000). Genes dependent on zebrafish cyclops function identified by AFLP differential gene expression screen. *Genesis, 26*(1), 86-97. doi:10.1002/(sici)1526-968x(200001)26:1<86::aid-gene11>3.0.co;2-q

Schindler, Y. L., Garske, K. M., Wang, J., Firulli, B. A., Firulli, A. B., Poss, K. D., & Yelon, D. (2014). Hand2 elevates cardiomyocyte production during zebrafish heart development and regeneration. *Development, 141*(16), 3112-3122. doi:10.1242/dev.106336

Schoenebeck, J. J., Keegan, B. R., & Yelon, D. (2007). Vessel and blood specification override cardiac potential in anterior mesoderm. *Dev Cell, 13*(2), 254-267. doi:10.1016/j.devcel.2007.05.012

Schwenty-Lara, J., Nehl, D., & Borchers, A. (2019). The histone methyltransferase KMT2D, mutated in Kabuki syndrome patients, is required for neural crest cell formation and migration. *Hum Mol Genet*. doi:10.1093/hmg/ddz284

Schwenty-Lara, J., Nurnberger, A., & Borchers, A. (2019). Loss of function of Kmt2d, a gene mutated in Kabuki syndrome, affects heart development in Xenopus laevis. *Dev Dyn, 248*(6), 465-476. doi:10.1002/dvdy.39

Serrano, M. L. A., Demarest, B. L., Tone-Pah-Hote, T., Tristani-Firouzi, M., & Yost, H. J. (2019). Inhibition of Notch signaling rescues cardiovascular development in Kabuki Syndrome. *PLoS Biol, 17*(9), e3000087. doi:10.1371/journal.pbio.3000087

Shangguan, H., Su, C., Ouyang, Q., Cao, B., Wang, J., Gong, C., & Chen, R. (2019). Kabuki syndrome: novel pathogenic variants, new phenotypes and review of literature. *Orphanet J Rare Dis, 14*(1), 255. doi:10.1186/s13023-019-1219-x

Shi, Y., & Whetstine, J. R. (2007). Dynamic regulation of histone lysine methylation by demethylases. *Mol Cell, 25*(1), 1-14. doi:10.1016/j.molcel.2006.12.010

Shpargel, K. B., Starmer, J., Wang, C., Ge, K., & Magnuson, T. (2017). UTX-guided neural crest function underlies craniofacial features of Kabuki syndrome. *Proc Natl Acad Sci U S A, 114*(43), E9046-E9055. doi:10.1073/pnas.1705011114

Shpargel, K. B., Starmer, J., Yee, D., Pohlers, M., & Magnuson, T. (2014). KDM6 demethylase independent loss of histone H3 lysine 27 trimethylation during early embryonic development. *PLoS Genet, 10*(8), e1004507. doi:10.1371/journal.pgen.1004507

Southard-Smith, E. M., Kos, L., & Pavan, W. J. (1998). Sox10 mutation disrupts neural crest development in Dom Hirschsprung mouse model. *Nat Genet, 18*(1), 60-64. doi:10.1038/ng0198-60

Stein, A. B., Jones, T. A., Herron, T. J., Patel, S. R., Day, S. M., Noujaim, S. F., . . . Dressler, G. R. (2011). Loss of H3K4 methylation destabilizes gene expression patterns and physiological functions in adult murine cardiomyocytes. *J Clin Invest, 121*(7), 2641-2650. doi:10.1172/JCI44641

Stief, S. M., Hanneforth, A. L., Weser, S., Mattes, R., Carlet, M., Liu, W. H., . . . Spiekermann, K. (2020). Loss of KDM6A confers drug resistance in acute myeloid leukemia. *Leukemia, 34*(1), 50-62. doi:10.1038/s41375-019-0497-6

Talbot, J. C., Johnson, S. L., & Kimmel, C. B. (2010). hand2 and Dlx genes specify dorsal, intermediate and ventral domains within zebrafish pharyngeal arches. *Development, 137*(15), 2507-2517. doi:10.1242/dev.049700

Tang, W., Martik, M. L., Li, Y., & Bronner, M. E. (2019). Cardiac neural crest contributes to cardiomyocytes in amniotes and heart regeneration in zebrafish. *Elife, 8*. doi:10.7554/eLife.47929

Tekendo-Ngongang, C., Kruszka, P., Martinez, A. F., & Muenke, M. (2019). Novel heterozygous variants in KMT2D associated with holoprosencephaly. *Clin Genet, 96*(3), 266-270. doi:10.1111/cge.13598

Teng, L., Mundell, N. A., Frist, A. Y., Wang, Q., & Labosky, P. A. (2008). Requirement for Foxd3 in the maintenance of neural crest progenitors. *Development, 135*(9), 1615-1624. doi:10.1242/dev.012179

Uy, B. R., Simoes-Costa, M., Koo, D. E., Sauka-Spengler, T., & Bronner, M. E. (2015). Evolutionarily conserved role for SoxC genes in neural crest specification and neuronal differentiation. *Dev Biol, 397*(2), 282-292. doi:10.1016/j.ydbio.2014.09.022

Van Laarhoven, P. M., Neitzel, L. R., Quintana, A. M., Geiger, E. A., Zackai, E. H., Clouthier, D. E., . . . Shaikh, T. H. (2015). Kabuki syndrome genes KMT2D and KDM6A: functional analyses demonstrate critical roles in craniofacial, heart and brain development. *Hum Mol Genet, 24*(15), 4443-4453. doi:10.1093/hmg/ddv180

Vincent, S. D., Mayeuf-Louchart, A., Watanabe, Y., Brzezinski, J. A. t., Miyagawa-Tomita, S., Kelly, R. G., & Buckingham, M. (2014). Prdm1 functions in the mesoderm of the second heart field, where it interacts genetically with Tbx1, during outflow tract morphogenesis in the mouse embryo. *Hum Mol Genet, 23*(19), 5087-5101. doi:10.1093/hmg/ddu232

Vissers, L. E., van Ravenswaaij, C. M., Admiraal, R., Hurst, J. A., de Vries, B. B., Janssen, I. M., . . . van Kessel, A. G. (2004). Mutations in a new member of the chromodomain gene family cause CHARGE syndrome. *Nat Genet, 36*(9), 955-957. doi:10.1038/ng1407

Walport, L. J., Hopkinson, R. J., Vollmar, M., Madden, S. K., Gileadi, C., Oppermann, U., . . . Johansson, C. (2014). Human UTY(KDM6C) is a male-specific N-methyl lysyl demethylase. *J Biol Chem, 289*(26), 18302-18313. doi:10.1074/jbc.M114.555052

Wang, L., & Shilatifard, A. (2019). UTX Mutations in Human Cancer. *Cancer Cell, 35*(2), 168-176. doi:10.1016/j.ccell.2019.01.001

Wang, Y. R., Xu, N. X., Wang, J., & Wang, X. M. (2019). Kabuki syndrome: review of the clinical features, diagnosis and epigenetic mechanisms. *World J Pediatr, 15*(6), 528-535. doi:10.1007/s12519-019-00309-4

Westerfield, M. (2000). *The Zebrafish Book: A Guide for the Laboratory Use of Zebrafish (Danio Rerio)*: University of Oregon Press.

Willaredt, M. A., Gorgas, K., Gardner, H. A., & Tucker, K. L. (2012). Multiple essential roles for primary cilia in heart development. *Cilia, 1*(1), 23. doi:10.1186/2046-2530-1-23

Wu, L., Wary, K. K., Revskoy, S., Gao, X., Tsang, K., Komarova, Y. A., . . . Malik, A. B. (2015). Histone Demethylases KDM4A and KDM4C Regulate Differentiation of Embryonic Stem Cells to Endothelial Cells. *Stem Cell Reports, 5*(1), 10-21. doi:10.1016/j.stemcr.2015.05.016

Xin, C., Wang, C., Wang, Y., Zhao, J., Wang, L., Li, R., & Liu, J. (2018). Identification of novel KMT2D mutations in two Chinese children with Kabuki syndrome: a case report and systematic literature review. *BMC Med Genet, 19*(1), 31. doi:10.1186/s12881-018-0545-5

Yang, L., Soonpaa, M. H., Adler, E. D., Roepke, T. K., Kattman, S. J., Kennedy, M., . . . Keller, G. M. (2008). Human cardiovascular progenitor cells develop from a KDR+ embryonic-stem-cell-derived population. *Nature, 453*(7194), 524-528. doi:10.1038/nature06894

Yang, Y., Hao, H., Wu, X., Guo, S., Liu, Y., Ran, J., . . . Zhou, J. (2019). Mixed-lineage leukemia protein 2 suppresses ciliary assembly by the modulation of actin dynamics and vesicle transport. *Cell Discov, 5*, 33. doi:10.1038/s41421-019-0100-3

Yap, C. S., Jamuar, S. S., Lai, A. H. M., Tan, E. S., Ng, I., Ting, T. W., & Tan, E. C. (2020). Identification of KMT2D and KDM6A variants by targeted sequencing from patients with Kabuki syndrome and other congenital disorders. *Gene, 731*, 144360. doi:10.1016/j.gene.2020.144360

Zhang, Q. J., Chen, H. Z., Wang, L., Liu, D. P., Hill, J. A., & Liu, Z. P. (2011). The histone trimethyllysine demethylase JMJD2A promotes cardiac hypertrophy in response to hypertrophic stimuli in mice. *J Clin Invest, 121*(6), 2447-2456. doi:10.1172/JCI46277

Zhang, Q. J., & Liu, Z. P. (2015). Histone methylations in heart development, congenital and adult heart diseases. *Epigenomics, 7*(2), 321-330. doi:10.2217/epi.14.60

Zhang, Y., Li, S., Yuan, L., Tian, Y., Weidenfeld, J., Yang, J., . . . Morrisey, E. E. (2010). Foxp1 coordinates cardiomyocyte proliferation through both cell-autonomous and nonautonomous mechanisms. *Genes Dev, 24*(16), 1746-1757. doi:10.1101/gad.1929210

Figure Legends

Figure 1: CRISPR/Cas9-mediated disruption of *kmt2d* and *kdm6a*/*l* results in frameshift mutations leading to alterations in cardiac morphology and global levels of H3K4me3 and H3K27me3, reduced heart rates, along with reduced heart rates.

A. Top: Schematic for zebrafish Kmt2d protein derived from UniProt showing various domains. Bottom: Schematic for zebrafish *kmt2d* gene showing CRISPR target region. Pink arrow shows CRISPR target site in both. Wild-type and two mutant alleles with corresponding ORF lengths are shown. Fonts: Pink – CRISPR target site, Red – stop codon, green – PAM (protospacer adjacent motif) sequence, dashes (-) – deletion, periods (….) – continuation. Abbreviations: aa – amino acids, bp – base pairs, CDS – coding sequence, ORF – open reading frame, PHD – plant homeodomain, FYRC – Phenylalanine Tyrosine – rich domain C-terminal, SET - Su(var)3-9, Enhancer-of-zeste and Trithorax.

B and C. Top: Schematic for zebrafish Kdm6a and Kdm6al protein derived from UniProt showing various domains. Bottom: Schematic for zebrafish *kdm6a*/*l* gene showing CRISPR target region. Pink arrow shows CRISPR target site in both. Wild-type and two mutant alleles with corresponding ORF lengths are shown. Fonts: Pink – CRISPR target site, Red – stop codon, green – PAM (protospacer adjacent motif) sequence, dashes (-) – deletion, periods (….) – continuation. Abbreviations: aa – amino acids, bp – base pairs, CDS – coding sequence, ORF – open reading frame, TPR - tetratricopeptide repeat, JmjC – Jumonji C.

D. *In situ* hybridization showing mRNA expression of *kmt2d*, *kdm6a*, and *kdm6al* in wild-type (top) and corresponding mutants (bottom) at 48 hpf (hours post fertilization). Lateral views are shown with anterior to left, scale 250 µm. Mutants were observed in Mendelian ratios of n=7/29 for *kmt2d*, n=8/31 for *kdm6a*, and n=7/30 for *kdm6al*.

E. Western blots for global levels of H3K4me3 and H3K27me3 with H3 control at 48 hpf wild-type and corresponding mutants as labeled. Quantification of band density shows a significant reduction using a Student's T-test * is $p<0.05$

F. Immunofluorescence for antibody staining of 48 hpf zebrafish, imaged by confocal microscopy. Red – MF20, green – *cmlc2*, blue – DAPI. Wild-type and corresponding mutants are indicated as labeled. Scale 75 µm. A- atrium, V - ventricle.

G. Quantification of heart beat rate using Student T-test $p<0.05$.

a, atrium; e, eye; h, heart; n, notochord; v, ventricle.

Figure 2: Expression of early cardiac marker genes are reduced in Kabuki Syndrome mutations.

In situ hybridization showing mRNA expressions of *hand2a* and *mef2ca* in wild-type and corresponding mutants at 48 hpf.

A, B. Ventral views are shown for *hand2a* and *mef2ca* expression in the developing zebrafish. Arrows, expression of *hand2* and *mef2ca* are especially reduced at the embryonic midline.

C. Lateral views for *mef2ca* show reduced expression in the heart field (arrowhead).

Scale 100 µm. Anterior to left for all images. e, eye; fb, fin bud; g, ganglion; h, heart; m, muscle; pas, pharyngeal arches. Mutants were observed in Mendelian ratios of n=8/34 for *kmt2d*, n=8/30 for *kdm6a*, n=7/29 for *kmd6al*, for *hand2a* expression, and n=7/30 for *kmt2d*, n=8/31 for *kdm6a*, n=8/33 for *kdm6al*, for *mef2ca* expression.

Figure 3: Expression of early neural crest-specific marker genes are reduced in Kabuki Syndrome mutations.

A, B. *In situ* hybridization showing mRNA expression of *sox10* and *foxd3* in wildtype embryos and corresponding mutants at 12 hpf and 14 hpf respectively. Dorsal views are shown for *sox10* and *foxd3* with scale 100 µm. Arrow, reduced expression of *foxd3* in the heart forming region of *kmt2d* and *kdm6a* mutants.

C. *crestin* expression at 24 hpf, and lateral views are shown for *crestin*, with scale 250 µm. Anterior to left for all images. e, eye; h, heart; nc, neural crest; y, yolk. Mutants were observed in Mendelian ratios of n=7/29 for *kmt2d*, n=8/29 for *kdm6a*, n=7/30 for *kdm6al*, for *sox10* expression; n=8/34 for *kmt2d*, n=8/31 for *kdm6a*, n=7/29 for *kdm6al*, for *foxd3* expression, and n=8/30 for *kmt2d*, n= 8/31 for *kdm6a*, n=7/30 for *kdm6al*, for *crestin* expression.

Figure 4: *KMT2D* shares common targets across humans, mice and zebrafish.

A. Table: Mutation information of patients.

B. Venn diagrams showing overlap between gene lists derived from RNA-sequencing (seq) analysis of *KMT2D* mutant datasets from humans, mice, and zebrafish as labeled.

C. Heat maps showing 76 common targets among human, mice, and zebrafish. Genes selected for RT-qPCR in Figure 4 C. are highlighted in green boxes.

D. RT-qPCR expression of 48 hpf zebrafish whole embryo mRNA of *sox12*, *slc22a23*, *foxp4*, *six3*, and *nr2f6a*, normalized with respect to *actb1*. Genes were selected from *KMT2D*'s common targets, based on their roles in cardiac and overall development. * - $p<0.05$, ** - $p<0.005$, ns - non-significant

Figure 5: *KMT2D* shares common targets across humans and various cell types of mice, which are similarly regulated in zebrafish.

A. Venn diagrams showing overlap between gene lists derived from RNA-seq analysis of *KDM6A* mutant datasets from humans and three distinct cell types of mice, as labeled.

B. Heat maps showing 7 common targets among human and 3 cell types of mice. Abbreviations: Ms – mouse, NCC – neural crest cells, NSC – neural stem cells, Cd4 – Cd4 T lymphocytes. Genes selected for RT-qPCR in Figure 5 C. are highlighted in green boxes.

C. RT-qPCR expression at 48 hpf zebrafish whole embryo mRNA of *id3*, *prdm1a*, and a*nxa4*, normalized with respect to *actb1*. Genes were selected from *KDM6A*'s common targets, based on their roles in cardiac and overall development. * - $p<0.05$, ** - $p<0.005$, ns - non-significant

Supplemental Figure 1: Quantification of heart area in Figure 1F shows no difference in overall heart size.

1027

1028

1029

1030

1031

1032

1033

1034

1035

1036

1037

1038

1039

1040

1041

1042

1043

1044

1045

1046

1047

1048

1049

1050

1051

1052

1053

1054

1055

1056

1057

1058

1059

1060

1061

1062

1063

1064

1065

1066

1067

1068

1069

1070

1071

1072

Figure 4: Table Gene Affected	Sex	Status	Effect at cDNA Level	Effect at Protein Level	Chromosomal Location (hg19)
KMT2D	♂	Proband	c.4288T>C	p.C1430R	chr12:47726789(hg18)
KDM6A	♀	Proband	Microdeletion, Gene deleted	Gene deleted	chrX:43620636-46881568

1091

1092

1093

1094

1095

1096

1097

1098

1099

1100

1101

1102

1103

1104

1105

1106

1107

1108

1109

1110

1111

1112

1113

A

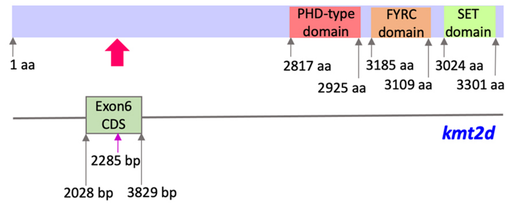

***kmt2d* Alleles:** **ORF lengths:**

wild-type: ATT GAG TTG AGG C----------AT AAT CCC AAA GGA TGC CA ... AAC TTC .... 9978 base pairs

allele 1: ATT GA--T TGA GGC GAG GCA TAA TTC CCA AAG GATG 1815 base pairs

allele 2: ATT GAG TTG AGG CAT AAT TCC CAA AGG ATG C ... TCT TGA 2115 base pairs

B

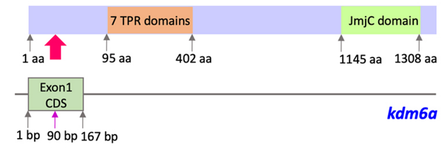

***kdm6a* Alleles:** **ORF lengths:**

wild-type: GGCGGGAAAAGCGAGAGAAACCGAGG...TTT TGC CAG TTA GGT... 4224 base pairs

allele 1: GGCGGGAAAAGCGAGAGAAACCGAGG...TGT TGT CCT CTA TAG 300 base pairs

wild-type: TGCTGCTGCTGG...GGCGGGAAAAGCGAGAGAAACCGAGG...TTT TGC CAG TTA GGT... 4224 base pairs

allele 2: TG---------G--TGG...GGCGGGAAAAGCGAGAGAAACCGAGG...TGT TGT CCT CTA TAG 300 base pairs

C

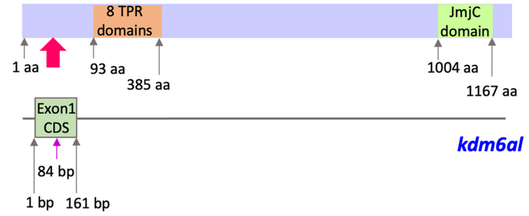

***kdm6al* Alleles:** **ORF lengths:**

wild-type: GGCGGGAAAAGCGAGTGAACCCGAGGAGGAATCACC....GCG TTG TCA... 4071 base pairs

allele 1: GGCGGGAAAAGCGA-TGAACCCGAGTGAGCGCACGGC....TAT TGA 336 base pairs

allele 2: GGCGGGAAAAGCGA-TGAACCCGAGACACAGCTCACT.....CCA TAG 342 base pairs

D

E

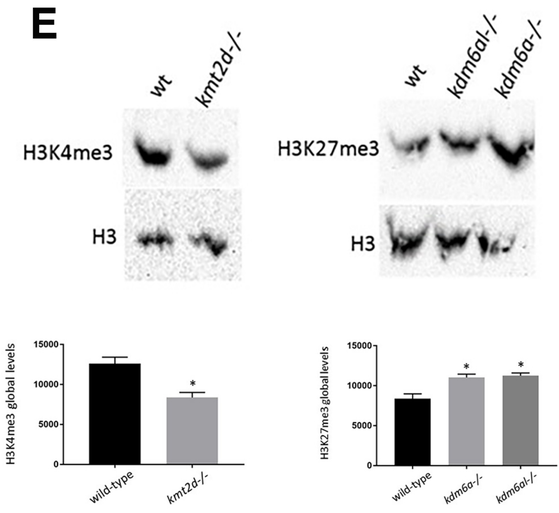

F

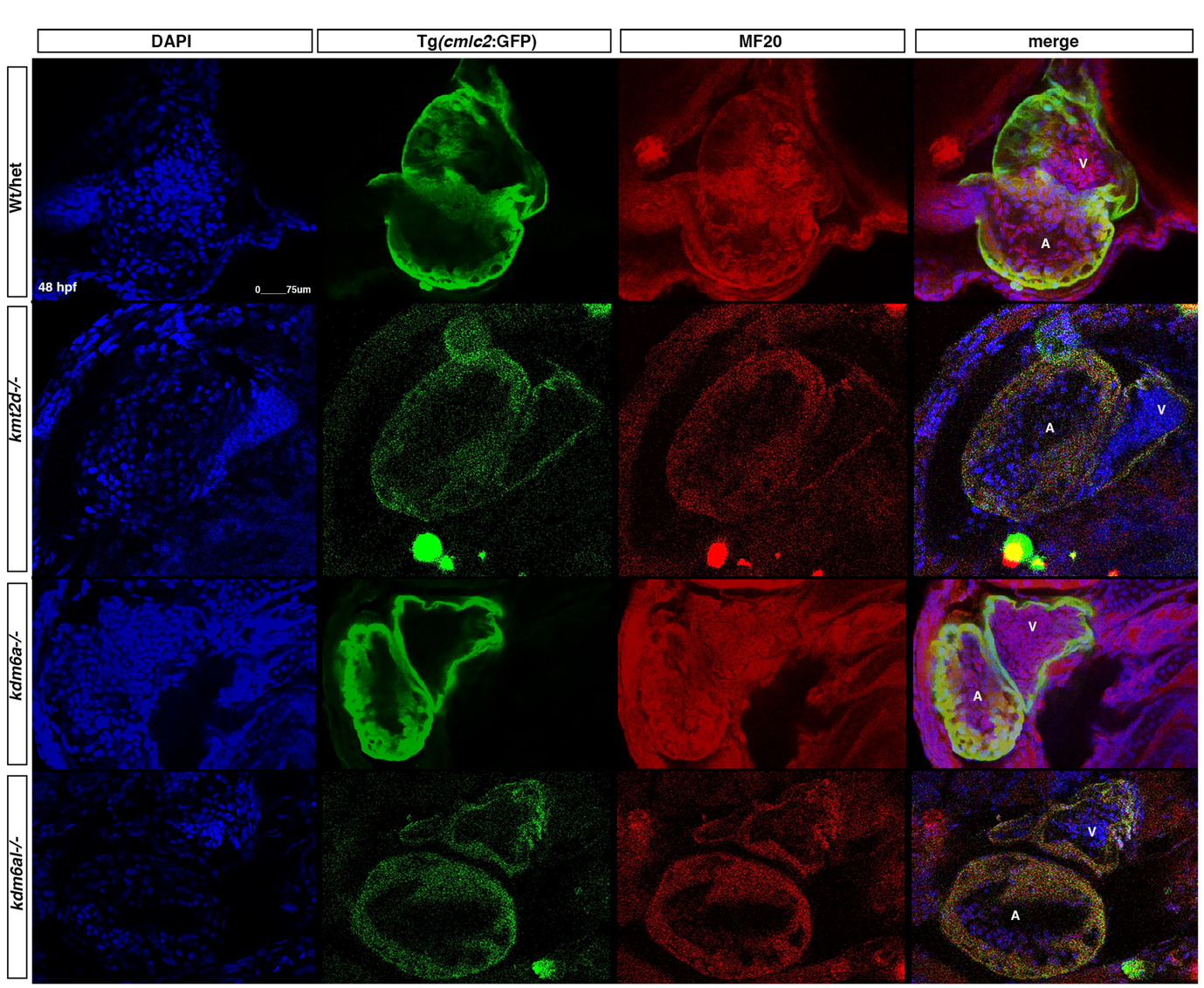

G

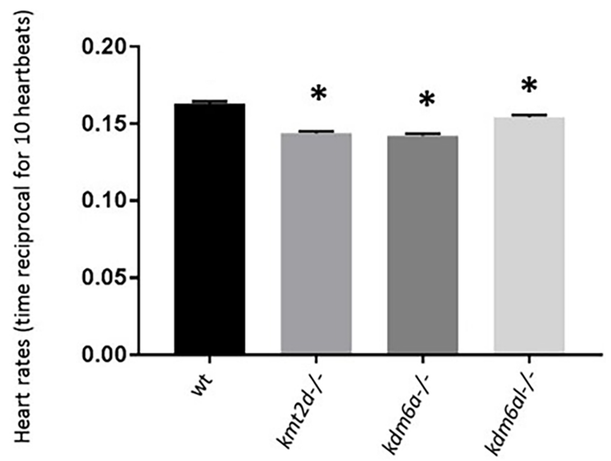

Sen et al Figure 1

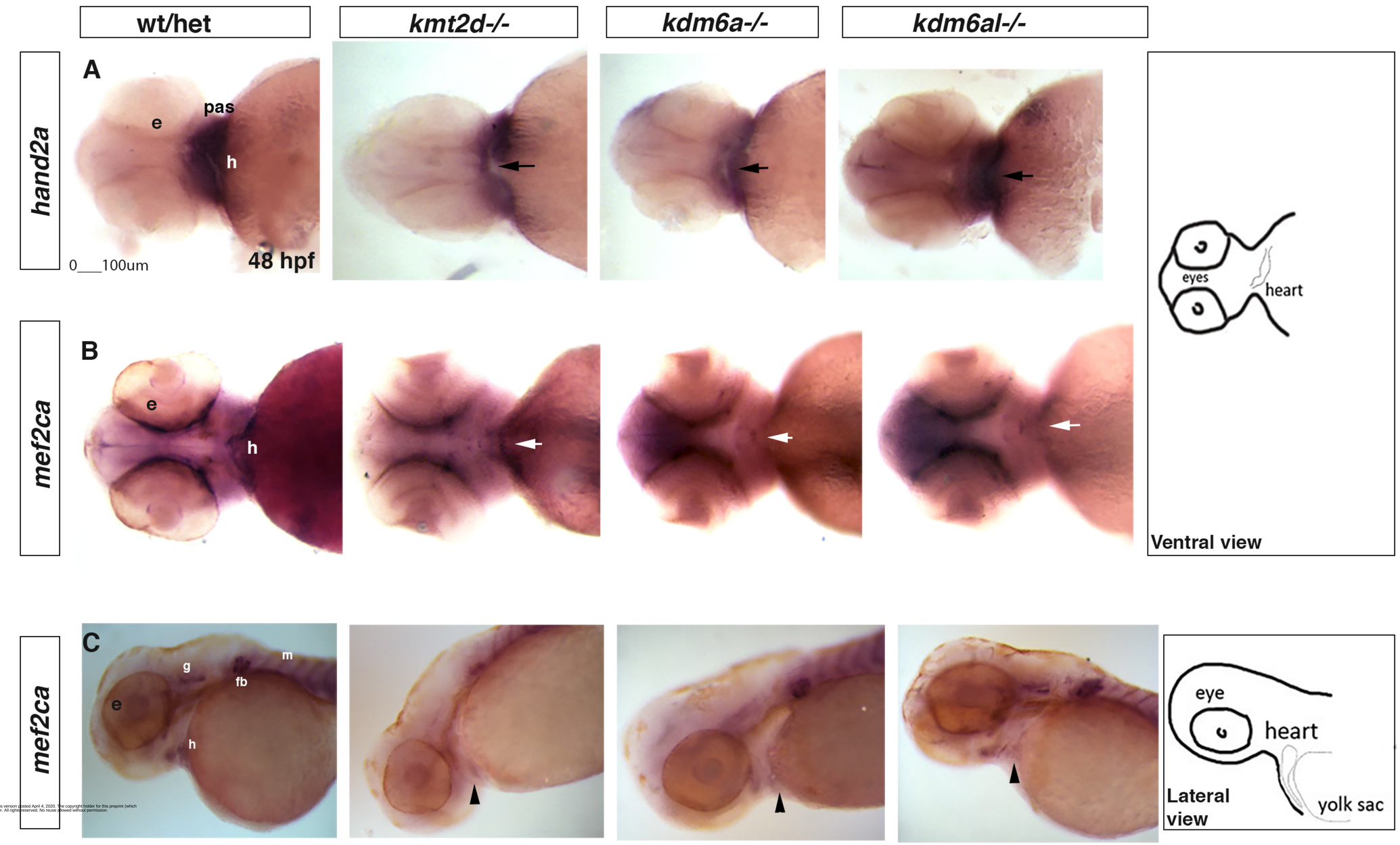

Sen et al Figure 2

Wt/het

kmt2d-/-

kdm6a-/-

kdm6al-/-

sox10

A

nc

0_____100um

12 hpf

foxd3

B

e

h

0_____100um

14 hpf

crestin

C

e

y

0_____250um

24 hpf

Sen et al Figure 3

A

Figure 4: Table Gene Affected	Sex	Status	Effect at cDNA Level	Effect at Protein Level	Chromosomal Location (hg19)
KMT2D	♂	Proband	c.4288T>C	p.C1430R	chr12:47726789(hg18)
KDM6A	♀	Proband	Microdeletion, Gene deleted	Gene deleted	chrX:43620636-46881568

B

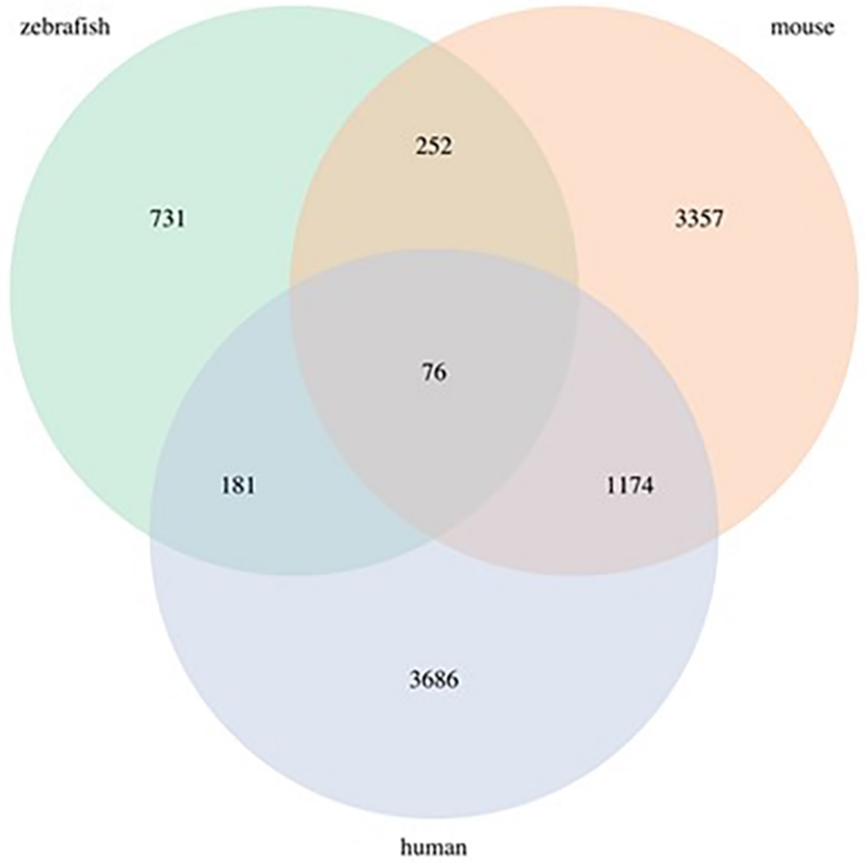

C

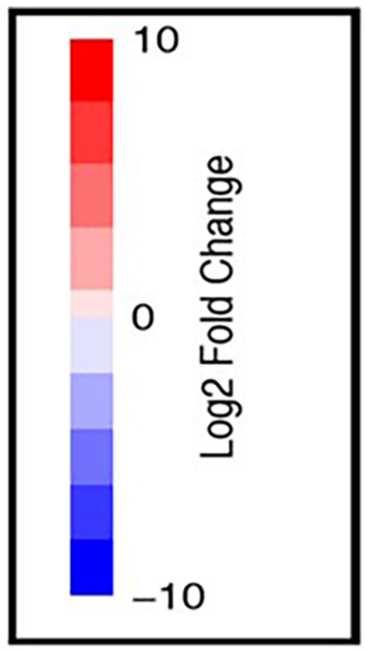

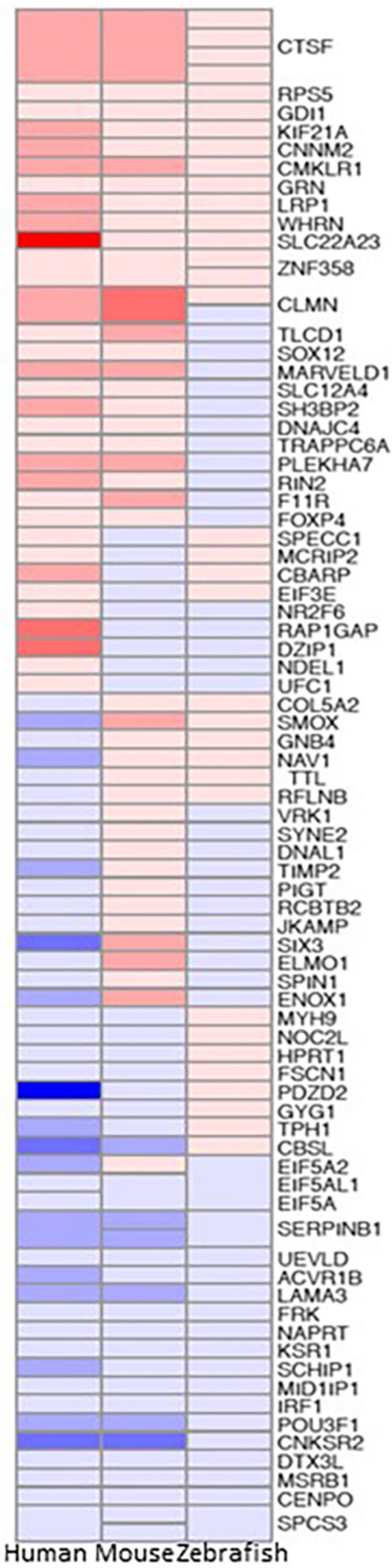

D

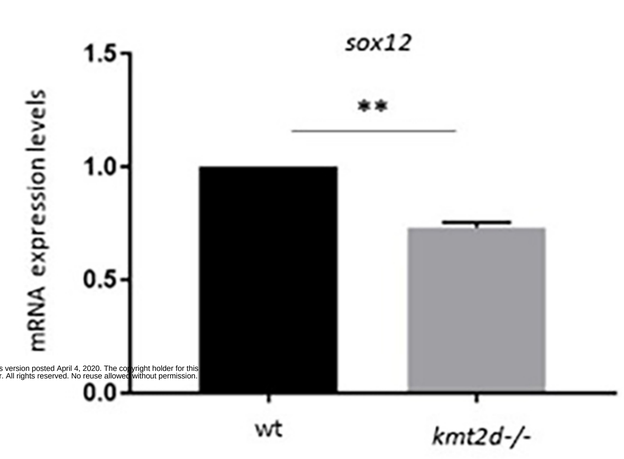

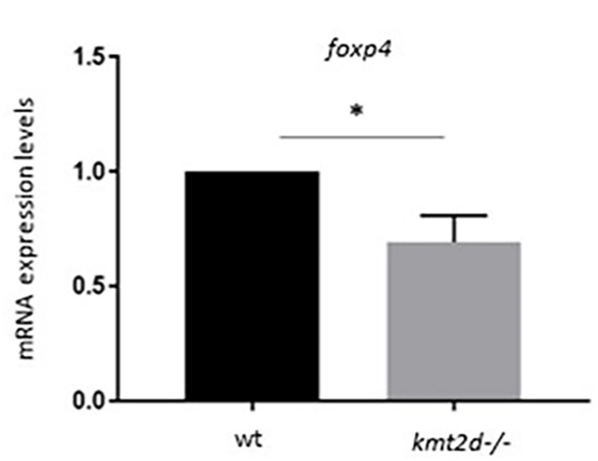

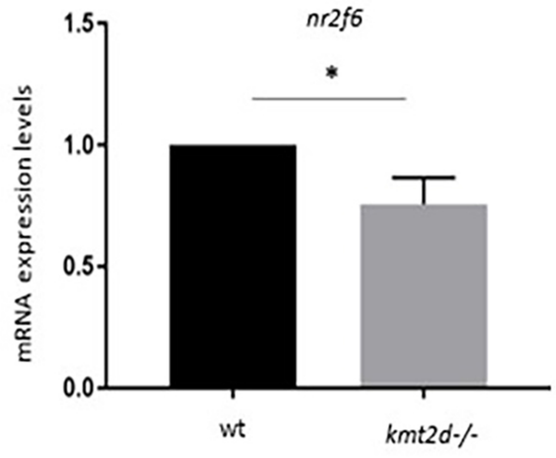

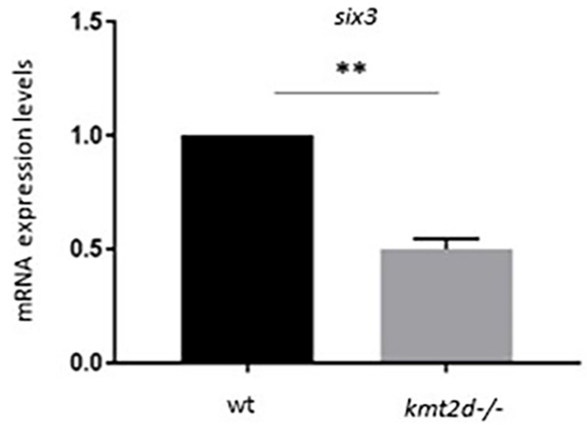

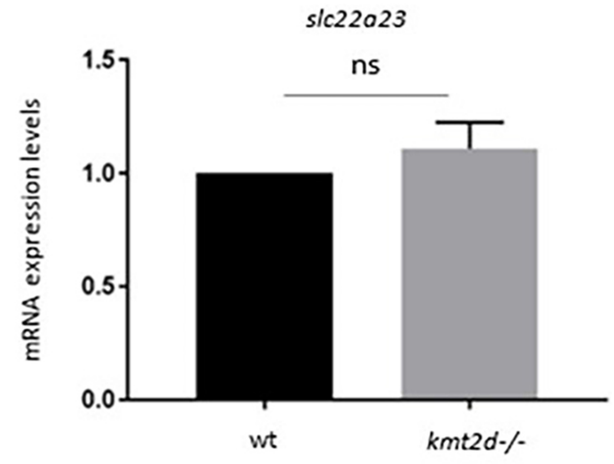

Sen et al Figure 4

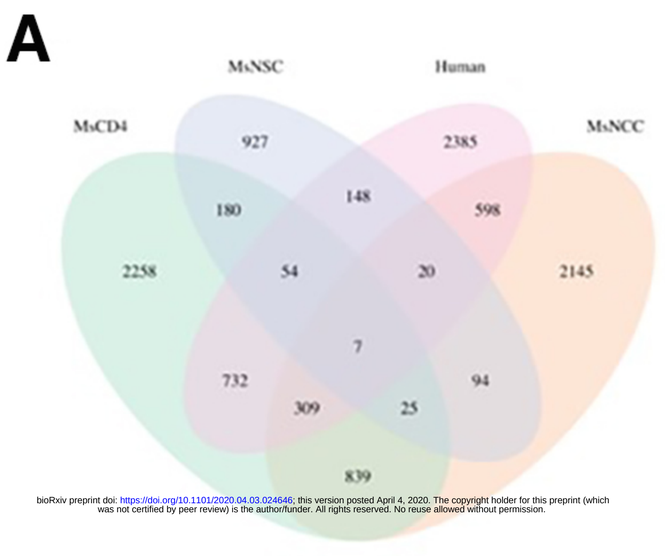

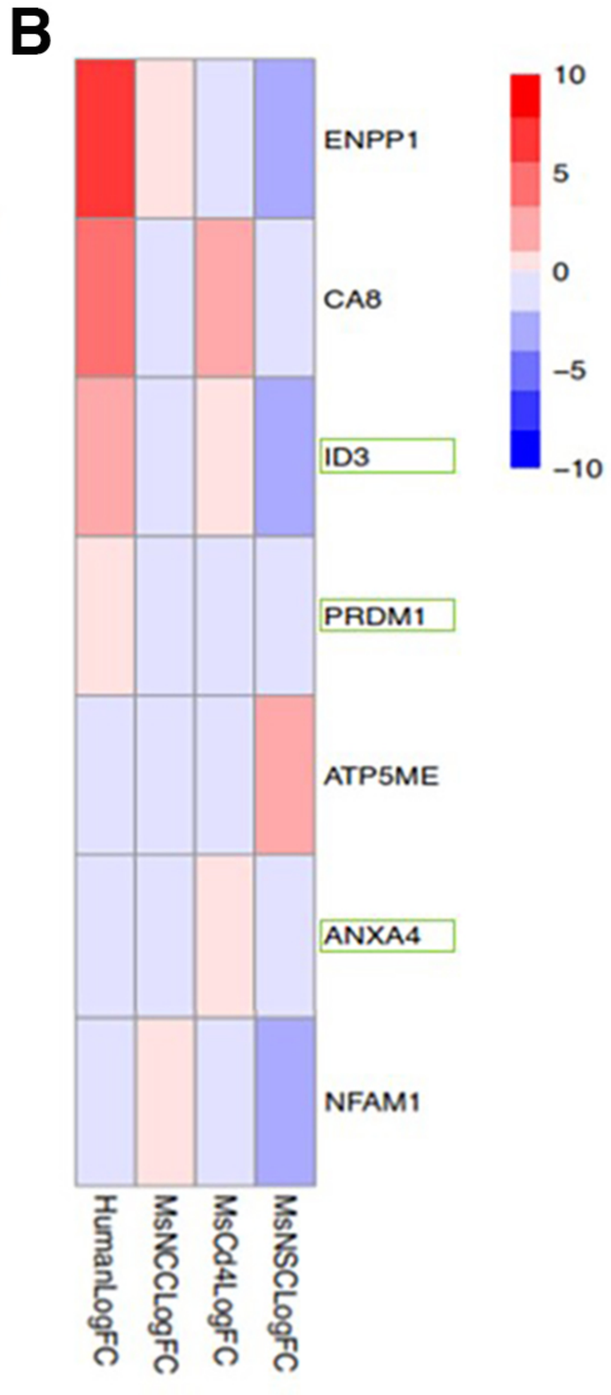

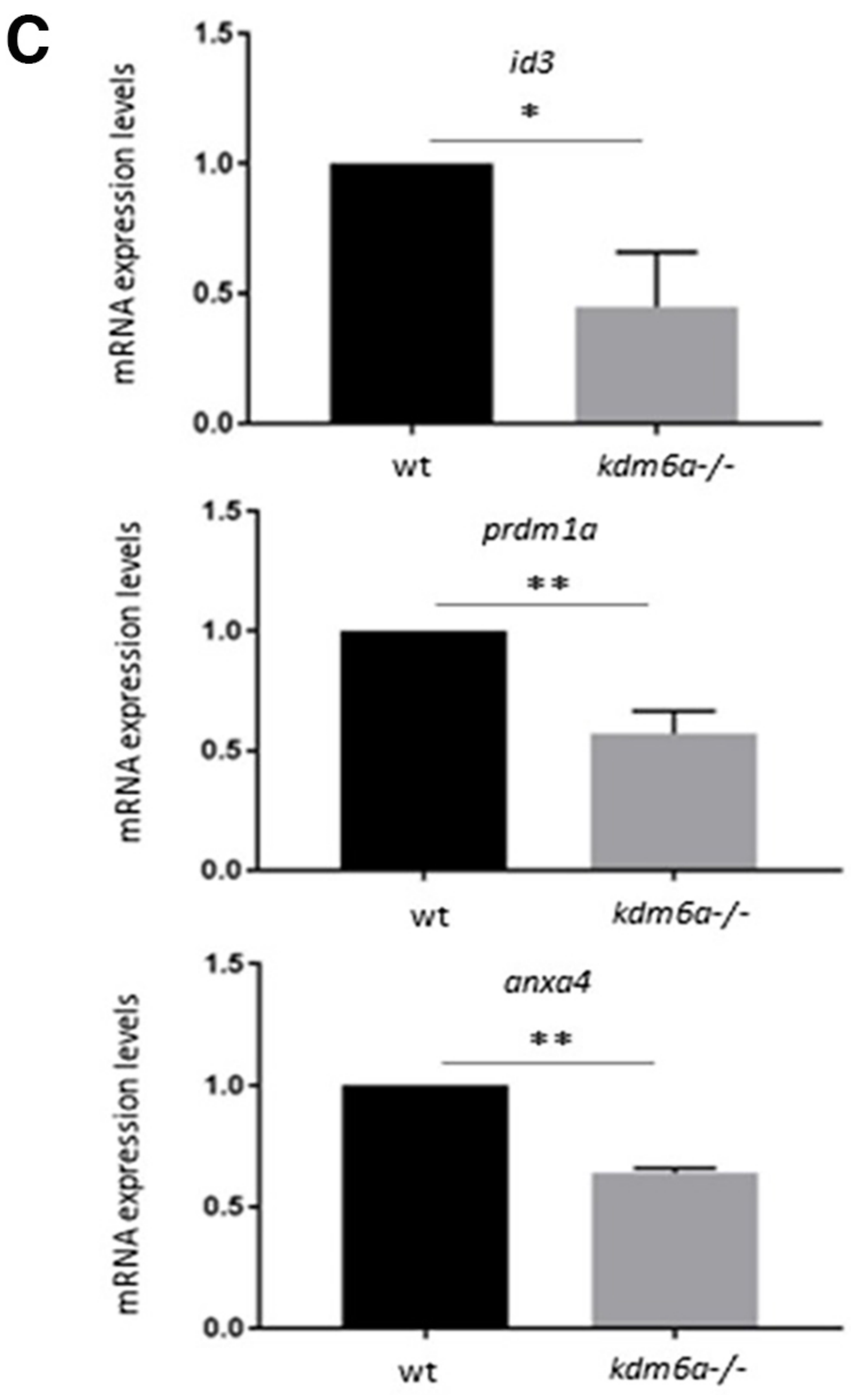

Sen et al Figure 5

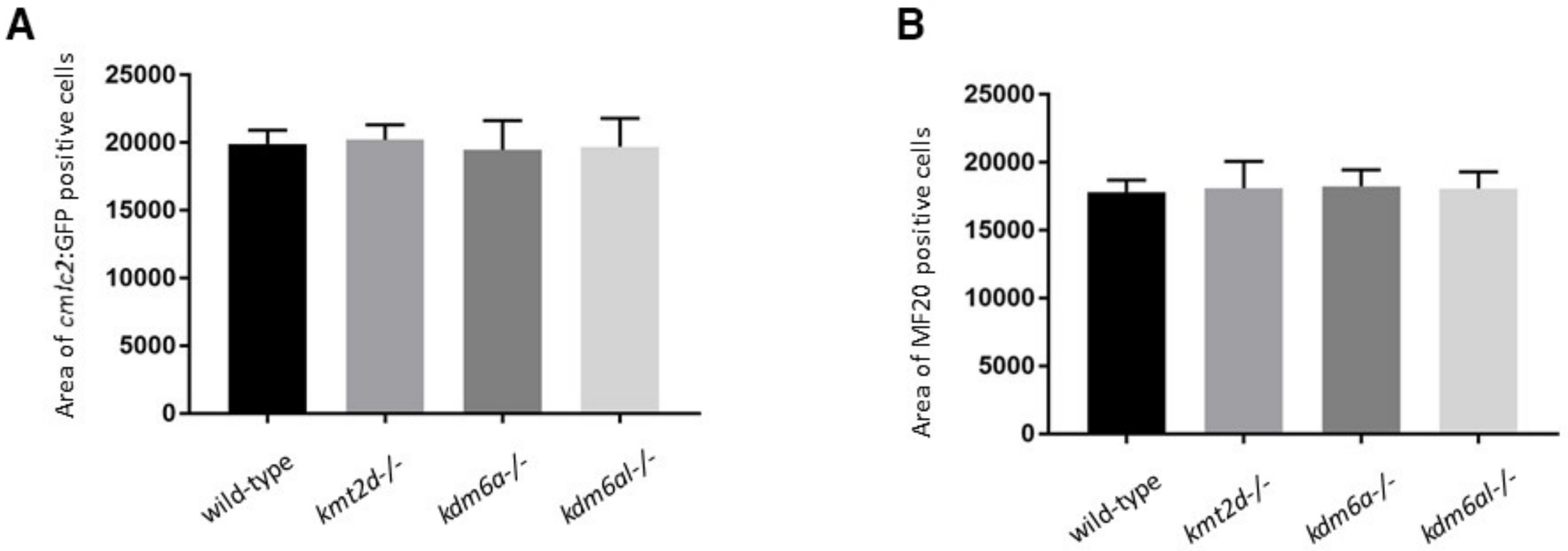

Sen et al, Supplemental Figure 1